

Identification of Celastramycin as a Novel Therapeutic Agent for Pulmonary Arterial Hypertension

High-Throughput Screening of 5562 Compounds

Ryo Kurosawa, Kimio Satoh, Nobuhiro Kikuchi, Haruhisa Kikuchi, Daisuke Saigusa, Md. Elias Al-Mamun, Mohammad A.H. Siddique, Junichi Omura, Taijyu Satoh, Shinichiro Sunamura, Masamichi Nogi, Kazuhiko Numano, Satoshi Miyata, Akira Uruno, Kuniyuki Kano, Yotaro Matsumoto, Takayuki Doi, Junken Aoki, Yoshiteru Oshima, Masayuki Yamamoto, Hiroaki Shimokawa

Rationale: Pulmonary arterial hypertension (PAH) is characterized by enhanced proliferation of pulmonary artery smooth muscle cells (PASMCs) accompanying increased production of inflammatory factors and adaptation of the mitochondrial metabolism to a hyperproliferative state. However, all the drugs in clinical use target pulmonary vascular dilatation, which may not be effective for patients with advanced PAH.

Objective: We aimed to discover a novel drug for PAH that inhibits PASM C proliferation.

Methods and Results: We screened 5562 compounds from original library using high-throughput screening system to discover compounds which inhibit proliferation of PASMCs from patients with PAH (PAH-PASMCs). We found that celastramycin, a benzoyl pyrrole-type compound originally found in a bacteria extract, inhibited the proliferation of PAH-PASMCs in a dose-dependent manner with relatively small effects on PASMCs from healthy donors. Then, we made 25 analogs of celastramycin and selected the lead compound, which significantly inhibited cell proliferation of PAH-PASMCs and reduced cytosolic reactive oxygen species levels. Mechanistic analysis demonstrated that celastramycin reduced the protein levels of HIF-1 α (hypoxia-inducible factor 1 α), which impairs aerobic metabolism, and κ B (nuclear factor- κ B), which induces proinflammatory signals, in PAH-PASMCs, leading to reduced secretion of inflammatory cytokine. Importantly, celastramycin treatment reduced reactive oxygen species levels in PAH-PASMCs with increased protein levels of Nrf2 (nuclear factor erythroid 2-related factor 2), a master regulator of cellular response against oxidative stress. Furthermore, celastramycin treatment improved mitochondrial energy metabolism with recovered mitochondrial network formation in PAH-PASMCs. Moreover, these celastramycin-mediated effects were regulated by ZFC3H1 (zinc finger C3H1 domain-containing protein), a binding partner of celastramycin. Finally, celastramycin treatment ameliorated pulmonary hypertension in 3 experimental animal models, accompanied by reduced inflammatory changes in the lungs.

Conclusions: These results indicate that celastramycin ameliorates pulmonary hypertension, reducing excessive proliferation of PAH-PASMCs with less inflammation and reactive oxygen species levels, and recovered mitochondrial energy metabolism. Thus, celastramycin is a novel drug for PAH that targets antiproliferative effects on PAH-PASMCs.

Visual Overview: An online visual overview is available for this article. (*Circ Res.* 2019;125:309-327. DOI: 10.1161/CIRCRESAHA.119.315229.)

Key Words: cell proliferation ■ energy metabolism ■ hypertension ■ hypoxia-inducible factor 1 ■ reactive oxygen species

Pulmonary arterial hypertension (PAH) is a fatal disease characterized by progressive obliteration of the vessel lumen and increased pulmonary artery pressure, leading to right ventricular (RV) failure and premature death.¹ During the past few decades, increased understanding of PAH

In This Issue, see p 259
Meet the First Author, see p 260

pathophysiology has led to the development of several effective therapies, including prostacyclin analogs and derivatives, endothelin receptor antagonists, PDE5 (phosphodiesterase

Received April 16, 2019; revision received June 7, 2019; accepted June 12, 2019.

From the Department of Cardiovascular Medicine (R.K., K.S., N.K., E.A.M., M.A.H.S., J.O., T.S., S.S., M.N., K.N., S.M., H.S.) Department of Integrative Genomics, Tohoku University Tohoku Medical Megabank Organization (D.S., A.U., M.Y.), and Department of Medical Biochemistry, Tohoku University Graduate School of Medicine (D.S., A.U., M.Y.), Sendai, Japan; Japan Society for the Promotion of Science, Tokyo, Japan (R.K.); and Tohoku University Graduate School of Pharmaceutical Sciences, Sendai, Japan (H.K., K.K., Y.M., T.D., J.A., Y.O.).

The online-only Data Supplement is available with this article at <https://www.ahajournals.org/doi/suppl/10.1161/CIRCRESAHA.119.315229>.

Correspondence to Hiroaki Shimokawa, MD, PhD, Department of Cardiovascular Medicine, Tohoku University Graduate School of Medicine, 1-1 Seiryomachi, Aoba-ku, Sendai 980-8574, Japan. Email shimo@cardio.med.tohoku.ac.jp

© 2019 American Heart Association, Inc.

Circulation Research is available at <https://www.ahajournals.org/journal/res>

DOI: 10.1161/CIRCRESAHA.119.315229

Novelty and Significance

What Is Known?

- Pulmonary arterial smooth muscle cells (PASMCs) from patients with pulmonary arterial hypertension (PAH) rigorously proliferate like cancer cells and finally occlude the distal pulmonary arteries, which is associated with increased production of inflammatory factors and adaptation of mitochondrial metabolism to a hyperproliferative state.
- Celastramycin is a benzoyl pyrrole-type compound originally found in a bacterial extract which suppresses NF- κ B (nuclear factor κ B)-like transcriptional factors.

What New Information Does This Article Contribute?

- Celastramycin inhibits cell proliferation of PASMCs from patients with PAH dose-dependently with small effects on control PASMCs. Celastramycin also inhibits inflammation and reactive oxygen species and recovers mitochondrial energy metabolism.
- Treatment with celastramycin ameliorates pulmonary hypertension in rodent models.

- Celastramycin is a promising drug for the treatment of patients with PAH that targets antiproliferative effects on PAH-PASMCs.

To our knowledge, this is the first study demonstrating that celastramycin inhibits cell proliferation of PASMCs from patients with PAH and ameliorates pulmonary hypertension in rodent models. We screened 5562 compounds from an original library using high-throughput screening and found celastramycin as a promising drug for PAH. Mechanistic analysis demonstrated that celastramycin reduces excessive proliferation of PASMCs from patients with PAH with changes in HIF-1 α (hypoxia-inducible factor 1 α), NF- κ B, and Nrf2 (nuclear factor erythroid 2-related factor 2), leading to less inflammation and reduced reactive oxygen species level and recovered mitochondrial energy metabolism. Furthermore, we showed that these celastramycin-mediated effects are regulated by the ZFC3H1 (zinc finger C3H1 domain-containing protein), a binding partner of celastramycin. Thus, the findings set the stage for further investigating the use of celastramycin for treatment of patients with PAH.

Nonstandard Abbreviations and Acronyms

AMPK	AMP-activated protein kinase
BRD4	bromodomain-containing protein 4
CO	cardiac output
DDI	Drug Discovery Initiative
ECAR	extracellular acidification rate
eNOS	endothelial NO synthase
GSSG	oxidized glutathione
HIF-1α	hypoxia-inducible factor 1 α
Keap1	Kelch-like ECH-associated protein 1
NF-κB	nuclear factor- κ B
Nrf2	nuclear factor erythroid 2-related factor 2
OCR	oxygen consumption rate
PAECs	pulmonary artery endothelial cells
PAH	pulmonary arterial hypertension
PAH-PAECs	PAECs from patients with PAH
PAH-PASMCs	PASMCs from patients with PAH
PARP-1	poly (ADP-ribose) polymerase-1
PASMCs	pulmonary artery smooth muscle cells
PDH	pyruvate dehydrogenase
PDK1	pyruvate dehydrogenase lipoamide kinase isozyme 1
PGC-1α	peroxisome proliferator-activated receptor γ co-activator 1- α
PH	pulmonary hypertension
PPARA	peroxisome proliferator-activated receptor- α
PPARD	peroxisome proliferator-activated receptor- δ
ROS	reactive oxygen species
RVSP	right ventricular systolic pressure
SDHA	succinate dehydrogenase complex subunit A
TFAM	mitochondrial transcription factor A
ZFC3H1	zinc finger C3H1 domain-containing protein

efficacy in patients with advanced PAH.⁴ Indeed, despite the improvements in treatment options, overall survival still remains unsatisfactory.⁵ Thus, it is important to develop novel drugs that possess different mechanisms of action.

It is known that the characteristics of pulmonary artery smooth muscle cells (PASMCs) from patients with PAH (PAH-PASMCs) are different from those from healthy controls (control PASMCs).¹ Indeed, PAH-PASMCs rigorously and continuously proliferate like cancer cells and finally occlude the distal pulmonary resistant vessels.⁶ Thus, effective treatment that achieves reverse remodeling needs to be developed for patients with advanced PAH. When we consider the abnormal phenotype of excessive proliferation⁷ and apoptosis-resistance⁸ in PAH-PASMCs, the abnormal phenotype itself can be a target for the development of novel drugs.⁹ Recently, the Drug Discovery Initiative (DDI) has been founded in Japan as a hub of the national collaborative research network for drug discovery, which provides consultation, technical assistance, and public chemical samples to researchers who will begin chemical screening (<http://www.ddi.u-tokyo.ac.jp/en/>).¹⁰ Tohoku University, a screening and library point of the DDI, has a unique library containing 5562 original compounds and automated machines to perform high-throughput screening (<http://www.pford.med.tohoku.ac.jp/index.html>). Celastramycin is a benzoyl pyrrole-type compound originally found in a bacteria extract, which arose from functional screenings using an ex vivo culture system in *Drosophila*.^{11,12} Celastramycin attenuates TNF (tumor necrosis factor)- α -mediated induction of IL (interleukin)-6 and IL-8 in human endothelial cells and lung cancer cells.^{12,13} It is also known that inflammation promotes cell proliferation by up-regulation of cytokines/chemokines and growth factors, some of which directly affect cell proliferation, migration, and differentiation of PASMCs. In animal models of pulmonary hypertension (PH), inflammation precedes vascular remodeling, suggesting that altered immunity is one of the primary events in the development of PAH.¹⁴ Cytokines and growth factors increase reactive oxygen species (ROS), which augment inflammation again.¹⁵

type 5) inhibitors, and an sGC (soluble guanylate cyclase) stimulator.^{2,3} However, all the drugs in clinical use for PAH are essentially pulmonary vasodilators, which have limited

Mounting evidence has implicated oxidative stress as an important pathogenic mechanism in PAH. Additionally, most of the cytokines directly affect mitochondrial function in PASCs.^{9,16}

In the present study, we screened the original library of Tohoku University using a high-throughput screening system and discovered that cellastramycin inhibits PAH-PASC proliferation with anti-inflammatory and antioxidant effects, leading to the recovery of mitochondrial function and amelioration in 3 rodent models of PH. Our data suggest that cellastramycin is a novel and promising drug for the treatment of PAH.

Methods

Additional detailed methods are included in the [online-only Data Supplement](#). The data that support the findings of this study are available from the corresponding author on reasonable request.

Human Lung Samples

Lung tissues were obtained from patients at the time of lung transplantation or surgery for lung cancer at a site far from the tumor margins as previously described.^{17–19} All patients provided written informed consent for the use of their lung tissues for the present study.

Study Approval

All protocols using human specimens were approved by the Institutional Review Board of Tohoku University, Sendai, Japan (No. 2013-1-160). All animal experiments were performed in accordance with the protocols approved by the Tohoku University Animal Care and Use Committee (No. 2015-Kodo-007) based on the Animal Research: Reporting of In Vivo Experiments guideline.

High-Throughput Screening

We used the original libraries of Tohoku University containing 5562 unique compounds in the DDI in Japan. PAH-PASCs were used for the first (proliferation assay) and second (repeatability assays, counter assays, and concentration-dependent assays) screening and control PASCs were used for counter assay (proliferation assay). We optimized screening conditions (cell number, time-course of plating cells, and adding stimulus) beforehand. PAH-PASCs were grown in DMEM with 10% FBS up to 80% confluency, which were plated at 1000 cells/45 μ L mediums in each well of a 384-well plate (Greiner Bio-One, Austria) using the Multidrop Combi (Thermo Fisher Scientific, Waltham). They were then placed in the automated incubator at 37°C for 24 hours. Diluted compounds (final concentration, 5 μ mol/L) were added to columns of every plate by the Biomek NX^P (Beckman Coulter, Brea, CA). The plates were incubated for additional 48 hours and evaluated by Cell Titer 96 Aqueous One Solution Cell Proliferation Assay kit (Promega) and the SpectraMax Paradigm (Molecular Devices). The intraplate and interplate variability showed a coefficient of variance of 5.9% and 4.0%, respectively.

Animal Experiments

All animal experiments were performed in accordance with the protocols approved by the Tohoku University Animal Care and Use Committee (No. 2015-Kodo-004) based on the Animal Research: Reporting of In Vivo Experiments guidelines and the recent recommendations with thorough randomization on the optimal preclinical studies in PAH.^{20,21} All the operations and analyses were performed in a blinded manner. We selected male rats because male rats were used in most previous studies as monocrotaline-induced PH or SUGEN/hypoxia-induced PH in rats, which are evidenced by accumulated papers with PH model animals.^{6,22} We were unable to conduct formal sample size and power calculations because the primary goal of this study was to explore the effect of an intervention (cellastramycin treatment) in vivo for the first time.

Statistical Analyses

All results are shown as mean \pm SEM. Comparisons of means between 2 groups were performed by unpaired Student *t* test for normally

distributed cases or the bootstrap method²³ for not normally distributed cases with unequal variances. Comparisons of means among ≥ 3 groups were performed by 1-way or 2-way ANOVA for normally distributed cases followed by the Tukey honestly significant difference method or the Dunnett method for multiple comparison, as appropriate. The normality of the underlying distributions was confirmed by the Shapiro-Wilk normality test. The multiplicity of the testing for not normally distributed cases was adjusted by the Holm method for pairwise 2-sample comparison.²⁴ Linear associations between 2 continuous variables were analyzed using linear regression model. The ratio of fully muscularized vessels was analyzed by the Poisson regression with the offset equals to the sum of total vessels with multcomp 1.4–6 package of R. Statistical significance was evaluated with GraphPad Prism 7.02 (GraphPad Software, Inc, La Jolla, CA), JMP 12 (SAS Institute Inc, Cary), or R version 3.3.2 (<http://www.R-project.org/>). All reported *P* values are 2-tailed, with a *P* value of <0.05 indicating statistical significance.^{17,25}

Results

Identification of Cellastramycin by High-Throughput Screening

To discover a novel drug for patients with severe PAH, we used the screening system of the DDI with 5562 original compounds and derivatives in the original chemical library of Tohoku University. For the screening procedure, we established cell libraries of primary cultured PAH-PASCs from patients undergoing lung transplantation and evaluated their inhibitory effects on cell proliferation after treatment with each compound (Figure 1A, Online Table I). We performed high-throughput screening to identify compounds that reduced proliferation of PAH-PASCs in a dose-dependent manner (Figure 1B). In the first screening, PAH-PASCs were incubated with each compound in 384-well plates for 24 hours. Among the compounds, we initially selected 80 that effectively inhibited PAH-PASC proliferation (Figure 1C). In the second screening, we performed repeatability assays and counter assays for the 80 compounds and selected 9 compounds that inhibited PAH-PASC proliferation with relatively small effects on control PASCs from healthy volunteers (Figure 1D, Online Figure I). Next, in the second screening, we performed a concentration-dependent assay for the 9 compounds in PAH-PASCs and control PASCs (Figure 1E). In the process of final selection, we also considered the existing information, which includes stability, toxicity, and complexity in each compound (Online Table II). Thus, we finally selected cellastramycin, as it has a promising structure and showed minimal effects on control PASCs. We further confirmed the antiproliferative effects of cellastramycin on PAH-PASCs in 6 different lines. Interestingly, inhibition rate of PAH-PASC proliferation positively correlated with the pulmonary vascular resistance in each patient (Online Figure II).

Because cardiac toxicity is an important issue when considering RV failure in patients with PAH, we confirmed that cellastramycin inhibits PAH-PASC proliferation without harmful effects on human adult cardiomyocytes (Online Figure IIIA). Interestingly, cellastramycin treatment downregulated the expression of brain natriuretic peptide (*NPPB*) in human adult cardiomyocytes compared with vehicle control (Online Figure IIIB). In contrast, cellastramycin treatment significantly upregulated the expressions of antioxidant genes, superoxide dismutase 2 (*SOD2*) and glutamate-cysteine ligase catalytic subunit (*GCLC*), in human adult

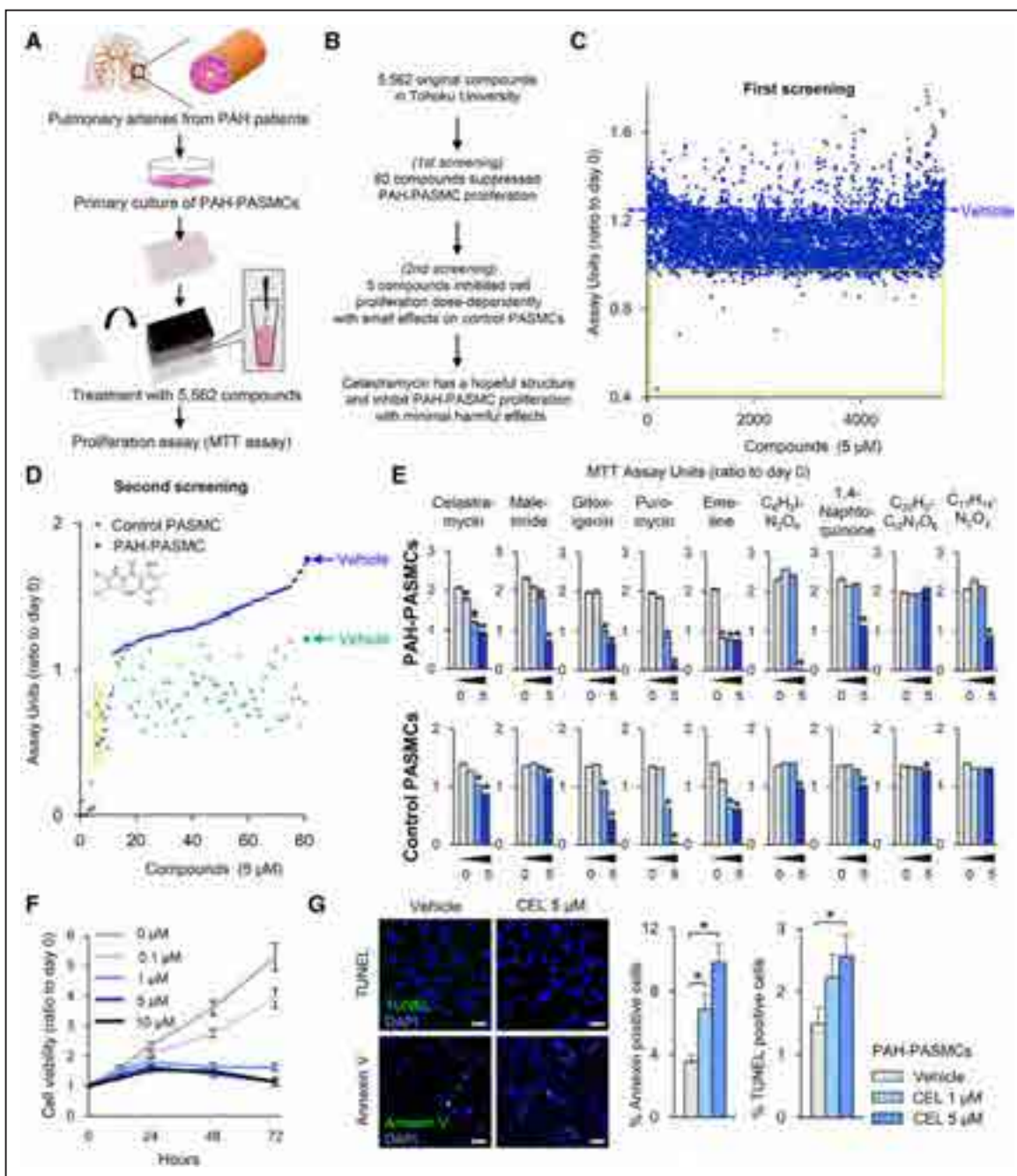


Figure 1. Screening of a novel compound that inhibits pulmonary artery smooth muscle cells from patients with pulmonary arterial hypertension (PAH-PASMC) proliferation. **A**, The schema of the primary culture of PAH-PASMCs and screening of the Tohoku University Compound Library (5562 compounds). **B**, Schematic outline of high-throughput screening to identify celestramycin (CEL) that inhibit PAH-PASMC proliferation with minimal harmful effects. **C**, Results of the first screening of 5562 compounds. The ratio of assay units by 3-(4,5-di-methylthiazol-2-yl)-2,5-diphenyltetrazolium bromide (MTT) assay after treatment with 5562 compounds (5 μmol/L) or vehicle for 24 h compared with day 0. Blue represents the MTT levels of PAH-PASMCs after treatment with 5562 compounds and we selected 80 compounds in the yellow square. **D**, Results of the second screening of 80 compounds. The ratio of assay units by MTT assay of PAH-PASMCs or PASMCs from healthy donors (control PASMCs) after treatment with 80 compounds (5 μmol/L) or vehicle for 48 h compared with day 0. Blue represents the MTT levels of PAH-PASMCs and green represents control PASMCs after treatment with 80 compounds and we selected CEL in the yellow square. **E**, Results of concentration-dependent assays with 9 compounds in PAH-PASMCs and control PASMCs. The ratio of assay units by MTT assay after treatment with different concentrations (0, 0.1, 1, and 5 μmol/L) of 9 compounds for 48 h as compared to day 0 (n=8 each). The 9 compounds are CEL, Maleimide, Gitoxigenin, Puromycin, Emetine, C₆H₃N₂O₄, 1,4-Naphthoquinone, C₂₂H₃₃N₇O₆, and C₁₁H₁₄N₂O₃. **F**, RealTime-Glo assay, in which cell viability was measured intermittently after treatment with different concentrations (0, 0.1, 1, 5, and 10 μmol/L) of CEL (n=8 each). **G**, Results of concentration-dependent apoptotic assays stained for Annexin V and TUNEL (terminal deoxynucleotidyl transferase-mediated dUTP nick-end labeling) in PAH-PASMCs after treatment with vehicle or CEL for 48 h (20 images/group). Scale bars, 50 μm. Data represent the mean±SEM. *P<0.05. Comparisons of parameters were performed with 1-way ANOVA followed by Dunnett test for multiple comparisons.

cardiomyocytes compared with vehicle control (Online Figure IIB). Moreover, we further performed experiments with pulmonary artery endothelial cells (PAECs) from patients with

PAH and control PAECs (Online Figure IV). Celestramycin treatment suppressed proliferation and apoptosis-resistance in PAECs from patients with PAH with relatively small

effects on control PAECs from healthy donors (Online Figure IVA and IVB). Indeed, it has been reported that PAECs from patients with PAH have highly proliferative and apoptosis-resistant features that induce occlusion of pulmonary arteries.²⁶ Moreover, celastramycin treatment significantly upregulated the eNOS (endothelial NO synthase) levels, which increase NO production in PAECs (Online Figure IVC).

Again, a cell variability assay confirmed that celastramycin exerts antiproliferative effects on PAH-PASMCs (Figure 1F). We also found that celastramycin minimally induced apoptosis, assessed by staining with Annexin V or TUNEL (terminal deoxynucleotidyl transferase-mediated dUTP nick-end labeling) in PAH-PASMCs (Figure 1G and Online Figure V). Thus, celastramycin is a novel drug that inhibits PAH-PASMC proliferation and induces apoptosis in a dose-dependent manner without harmful effects on normal PASMCs or cardiomyocytes.

Development of Celastramycin Analogues and Their Structure-Activity Correlation

To determine the antiproliferative structure of the celastramycin molecule, we developed 25 analogs and examined their antiproliferative effects on PAH-PASMCs. First, we synthesized 8 analogs with different lengths of alkyl chain (R; Figure 2A). These analogs had strong antiproliferative effects on PAH-PASMCs (Figure 2B). Interestingly, their antiproliferative effects depended on the length of R (Figure 2C). In contrast, substitution of R with a chlorine atom (Figure 2D) completely abolished the antiproliferative effects (Figure 2B). Next, we introduced a single modification in the basal common structure, e (Figure 2E), which slightly attenuated the antiproliferative effects on PAH-PASMCs (Figure 2B). Moreover, excessive modification of the basic common structure (Figure 2F) completely abolished the antiproliferative effects on PAH-PASMCs (Figure 2B). These results suggest the crucial role of the basal common structure for the antiproliferative effects on PAH-PASMCs. Importantly, celastramycin analogs with the basal common structure inhibited proliferation in different PAH-PASMC cell lines in a dose-dependent manner (Online Figure VI). Finally, we evaluated the levels of cytosolic ROS after treatment with the 25 analogs and found that the analog b significantly reduced ROS in PAH-PASMCs (Figure 2G). Because we previously confirmed that intracellular ROS in PAH-PASMCs is increased compared with control PASMCs¹⁹ and higher levels of cytosolic ROS are mechanistically involved in the proliferation of PAH-PASMCs,^{19,27,28} we used the analog b in the following experiments in vivo and in vitro.

Celastramycin Improves Mitochondrial Energy Metabolism in PAH-PASMCs

Abnormal activation of HIF-1 α (hypoxia-inducible factor 1 α) in normoxia is well known in PAH-PASMCs, which augments transcription of many genes promoting proproliferative signals, impaired oxidative glucose metabolism, and the shift to aerobic glycolysis.²⁹ Interestingly, celastramycin treatment reduced HIF-1 α mRNA (*HIF1A*) and increased glucose transporter 1 mRNA (*SLC2A1*) in PAH-PASMCs compared with vehicle controls (Figure 3A, Online VIIA). Importantly, HIF-1 α was upregulated in PAH-PASMCs compared with control PASMCs, and celastramycin treatment significantly reduced

protein levels of HIF-1 α in PAH-PASMCs compared with vehicle controls (Figure 3A). Additionally, celastramycin significantly reduced downstream PDK1 (pyruvate dehydrogenase lipoamide kinase isozyme 1), which inactivates PDH (pyruvate dehydrogenase) to converts pyruvic acid to acetyl CoA (coenzyme A), and DRP1 (dynamin-1-like protein) that promotes mitochondrial fission, both of which were upregulated in PAH-PASMCs compared with control PASMCs (Figure 3A). Moreover, celastramycin significantly reduced protein levels of Keap1 (Kelch-like ECH-associated protein 1), which suppresses Nrf2 (nuclear factor erythroid 2-related factor 2), in both PAH-PASMCs and control PASMCs (Figure 3B). Consistently, celastramycin increased protein levels of Nrf2 in nuclear extracts in PAH-PASMCs compared with vehicle controls (Figure 3B). Indeed, celastramycin upregulated the expression of Nrf2 (*NFE2L2*), a master regulator of cellular response against oxidative stress, and its downstream genes, NAD(P) H quinone dehydrogenase-1 (*NQO1*), heme oxygenase-1 (*HMOX1*), *GCLC*, and *SOD2* in PAH-PASMCs compared with vehicle controls (Figure 3C, Online Figure VIIB). Moreover, celastramycin significantly increased *SOD2* in total cell lysates compared with vehicle controls (Online Figure VIIC). Thus, we next focused on the role of celastramycin in altering the redox state in PAH-PASMCs. Indeed, we detected significantly higher levels of ROS in PAH-PASMCs compared with control PASMCs (Figure 3D). However, celastramycin treatment significantly reduced cytosolic ROS in PAH-PASMCs assessed by staining with CellROX and 2,7-dichlorodihydrofluorescein compared with vehicle controls (Figure 3D, Online Figure VIII). Consistently, NADPH oxidase activity was significantly higher in PAH-PASMCs compared with control PASMCs at baseline, which was significantly reduced by the celastramycin treatment (Figure 3E). Here, it has been demonstrated that NADPH oxidase regulates the activities of Nrf2 in several cell lines.^{30,31} Conversely, Keap1-Nrf2 pathway regulates the cytosolic ROS production through inhibition of NADPH oxidase.³² Indeed, celastramycin significantly reduced Keap1 and increased Nrf2 in PAH-PASMCs (Figure 3B). Thus, these reports and our data suggest that celastramycin downregulates Keap1 and upregulates Nrf2, contributing to the inhibition of NADPH oxidases in PAH-PASMCs. Next, to evaluate the antioxidant capacity of celastramycin, we evaluated levels of glutathione and oxidized glutathione (GSSG). To elicit antioxidant effects, glutathione is converted to GSSG, and only free glutathione has antioxidant effects. In contrast, GSSG lacks antioxidant functions and is a byproduct of the scavenging activity of glutathione. Thus, glutathione/GSSG ratio is important in assessing the total capacity of cytosolic ROS removal. Here, glutathione/GSSG ratio was significantly downregulated in PAH-PASMCs compared with control PASMCs, both of which were significantly increased by celastramycin treatment (Figure 3F). In contrast, celastramycin treatment significantly increased mitochondrial ROS (mROS) in PAH-PASMCs assessed by MitoSOX staining compared with vehicle controls (Figure 3G). Here, it is well known that dysregulated mitochondrial function and ATP production cause a decrease in the production of mROS in PAH-PASMCs.³³ Thus, we next examined the role of celastramycin on mitochondrial functions in PAH-PASMCs.

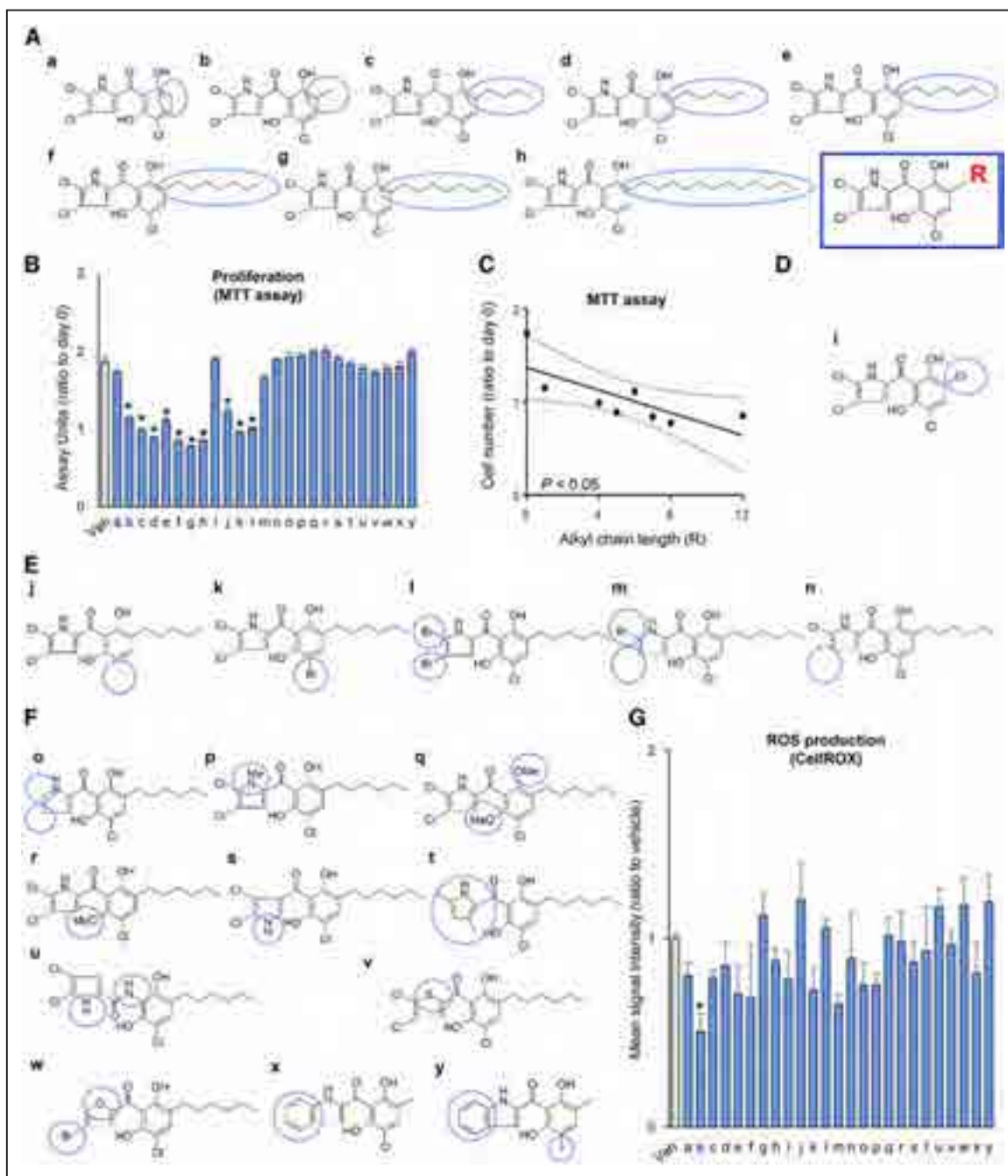


Figure 2. Celastramycin analogs and structure-activity correlation. **A**, The chemical structures of 8 analogs, a–h, with different lengths of alkyl chain (R). **B**, The ratio of cell numbers after treatment with 25 analogs for 48 h compared with day 0 ($1 \mu\text{mol/L}$, $n=8$ each). Cell numbers were measured by 3-(4,5-dimethylthiazol-2-yl)-2,5-diphenyltetrazolium bromide (MTT) assay. **C**, Structure-activity correlation between the length of the alkyl chain (R) and proliferation of pulmonary artery smooth muscle cells from patients with pulmonary arterial hypertension (PAH-PASMCs). **D**, The chemical structure of 1 analog, i, which substituted R into a chlorine atom. **E**, The chemical structures of 5 analogs, j–n, in which 1 or 2 branches in the basal common structure e were modified. **F**, The chemical structures of 11 analogs, o–y, in which the basal common structure e were excessively modified. **G**, The levels of reactive oxygen species (ROS) in PAH-PASMCs assessed by CellROX after treatment with the 25 analogs for 24 h ($n=3$ each). Data represent the mean \pm SEM. $*P<0.05$. Comparisons of parameters were performed with an unpaired Student *t* test or Dunnett test for multiple comparisons. Linear associations between 2 continuous variables were analyzed using a linear regression model.

Using a Seahorse XF24-3 apparatus, which provides information on mitochondrial functions through real-time measurements of oxygen consumption rate (OCR; a marker of oxidative phosphorylation) and extracellular acidification rate (ECAR; a surrogate for glycolysis), we evaluated the effects of celastramycin treatment on control PASMCs and

PAH-PASMCs (Figure 3H). OCR reflects the mitochondrial respiration rate and energy production, while ECAR the rate of glycolysis. Here, we observed significantly lower levels of ATP production, maximal respiration, and OCR/ECAR ratio in PAH-PASMCs compared with control PASMCs, which were significantly increased by the celastramycin treatment

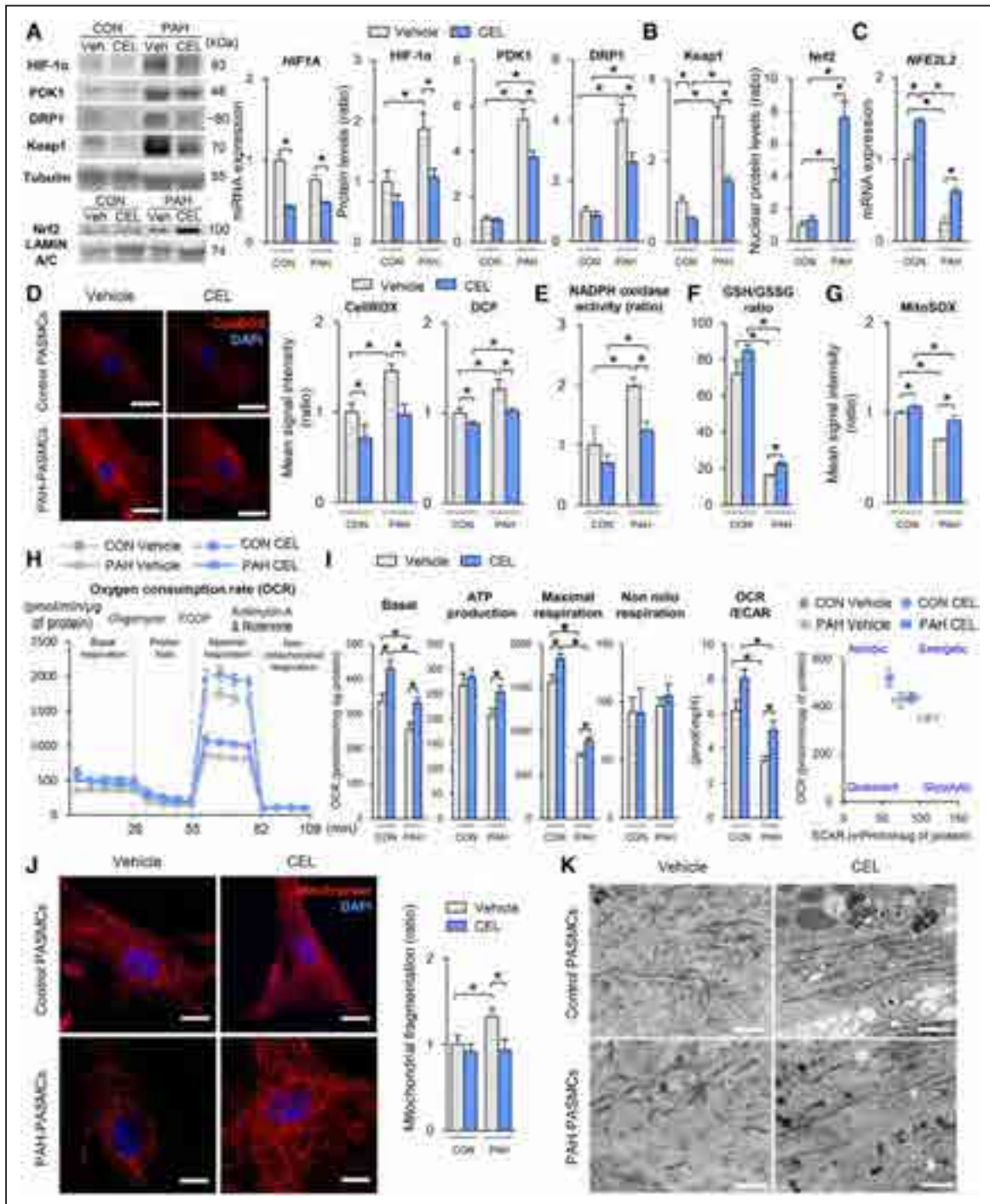


Figure 3. Celastramycin (CEL)-mediated recovery of mitochondrial functions in pulmonary artery smooth muscle cells from patients with pulmonary arterial hypertension (PAH-PASMCs). **A**, Real-time polymerase chain reaction (RT-PCR) analysis of HIF-1 α (hypoxia-inducible factor-1 α ; *HIF1A*) mRNA in control PASMCs and PAH-PASMCs after the treatment with CEL or the control vehicle for 24 h (n=6) and quantification of HIF-1 α , PDK1 (pyruvate dehydrogenase lipoamide kinase isozyme 1) and DRP1 (dynamin-1-like protein) in control PASMCs and PAH-PASMCs after the treatment with CEL or the control vehicle for 24 h (n=6). **B**, Quantification of Keap1 (Kelch-like ECH-associated protein 1) in total cell lysate and Nrf2 (nuclear factor erythroid 2-related factor 2) in nuclear extract of control PASMCs and PAH-PASMCs after the treatment with CEL or vehicle for 24 h (n=6). **C**, RT-PCR analysis of Nrf2 (*NFE2L2*) mRNA in control PASMCs and PAH-PASMCs after the treatment with CEL or the control vehicle for 24 h (n=6). **D**, **Left**, representative images of CellROX Deep Red fluorescence in control PASMCs and PAH-PASMCs. Nuclei were counterstained using DAPI (4',6-diamidino-2-phenylindole). Scale bars, 50 μ m. **Right**, quantification of CellROX and 2,7-dichlorodihydrofluorescein (DCF) fluorescence intensity in control PASMCs and PAH-PASMCs after the treatment with CEL or control vehicle for 24 h (n=8 each). **E**, Quantification of NADPH oxidase activity in control PASMCs and PAH-PASMCs after the treatment with CEL or the control vehicle for 12 h (n=8 each). **F**, Quantification of glutathione (GSH)/oxidized GSH (GSSG) ratio in control PASMCs and PAH-PASMCs after vehicle or CEL treatment for 4 h (n=8 each). **G**, Quantification of mitochondrial reactive oxygen species assessed by MitoSOX fluorescence intensity in control PASMCs and PAH-PASMCs after the treatment with CEL or the control vehicle for 24 h (n=8 each). **H**, Quantification of the mitochondrial oxygen consumption rate (OCR) of control PASMCs and PAH-PASMCs after the treatment with CEL or the control vehicle for 24 h (n=5). **I**, Quantification of the OCR of control PASMCs and PAH-PASMCs after the treatment with CEL or the control vehicle for 24 h (n=5 each). Oligomycin inhibits ATP synthase (complex V), and the decrease in OCR followed by oligomycin correlates to the mitochondrial respiration associated with cellular ATP production. (*Continued*)

Figure 3 Continued. Carbonyl cyanide-4 (trifluoromethoxy) phenylhydrazone is an uncoupling agent that disrupts the mitochondrial membrane potential. As a result, electron flow through the electron transport chain is uninhibited, and oxygen is maximally consumed by complex IV. Rotenone and antimycin A were injected to inhibit the flux of electrons through complex I and III, respectively, and thus shut down mitochondrial oxygen consumption. **J, Left,** representative images of control PASMCS and PAH-PASMCS labeled for mitochondria after the treatment with CEL or the control vehicle for 24 h. Nuclei were counterstained using DAPI. Scale bars, 20 μm . **Right,** quantification of mitochondrial fragmentation in control PASMCS and PAH-PASMCS labeled for mitochondria after the treatment with CEL or the control vehicle for 24 h. **K,** Representative transmission electron microscopy images of control PASMCS and PAH-PASMCS after the treatment with CEL or the control vehicle for 24 h. Scale bars, 2 μm . Data represent the mean \pm SEM. * P <0.05. Comparisons of parameters were performed with 2-way ANOVA, followed by Tukey honestly significant difference test for multiple comparisons. CON indicates control; ECAR, extracellular acidification rate; and Veh, vehicle.

(Figure 3I). Furthermore, PAH-PASMCS showed significantly increased glycolysis compared with control PASMCS, which was slightly reduced by the celastrol treatment (Online Figure IX). Thus, we next examined the morphologies of mitochondria in PAH-PASMCS after celastrol treatment for 24 hours. Importantly, celastrol treatment showed increased mitochondrial networks assessed using a MitoTracker in PAH-PASMCS compared with vehicle controls (Figure 3J, Online Figure X). Additionally, celastrol treatment showed increased mitochondrial networks assessed by transmission electron microscopy in PAH-PASMCS compared with vehicle controls (Figure 3K, Online Figure XI). Consistently, celastrol treatment significantly reduced the levels of DRP1 (dynamin-1-like protein) that promotes mitochondrial fission (Figure 3A). Moreover, celastrol increased the expressions of genes for mitochondrial fusion, such as mitofusin 1 (*MFN1*), mitofusin 2 (*MFN2*), and mitochondrial elongation factor (*MIEF1*) and reduced the expressions for mitochondrial fission, such as DRP1 (*DNM1L*), mitochondrial fission 1 protein (*FIS1*), and optic atrophy type 1 (*OPA1*) in PAH-PASMCS compared with vehicle controls (Online Figure VIII). Additionally, celastrol significantly upregulated the expressions of genes for mitochondrial biogenesis, such as PGC-1 α (peroxisome proliferator-activated receptor γ coactivator 1- α ; *PPARGC1A*), mitochondrial transcription factor A (*TFAM*), and nuclear respiratory factor 1 (*NRF1*) and genes for mitochondrial function, such as peroxisome proliferator-activated receptor- α and δ (*PPARA*, *PPARD*) in PAH-PASMCS compared with vehicle controls (Online Figure VIII). These results suggest that celastrol treatment affects the balance between mitochondrial biogenesis and functions, resulting in increased mitochondrial networks and mROS levels in PAH-PASMCS.

Celastrol-Mediated Changes in Metabolomics in PAH-PASMCS

It has been reported that circulating metabolites are dramatically altered in patients with PAH.³⁴ Additionally, metabolic profiles predicted the long-term prognosis of patients with PAH, suggesting that metabolic changes could be important modifiers of disease progression.³⁴ Based on the celastrol-mediated recovery in mitochondrial function, we hypothesized that celastrol may change metabolic profiles in PAH-PASMCS and their secreted proteins. Thus, we performed metabolomic analyses to evaluate the metabolic changes in PAH-PASMCS by the treatment with celastrol. Here, we used a broad metabolomics platform to analyze >400 metabolites in total cell lysates of PAH-PASMCS and compared the changes after the treatment with celastrol (Online Figure XIII). Interestingly, we found a dramatic change in several metabolites by celastrol treatment (Online Figure XIIB).

In agreement, celastrol treatment increased the levels of metabolite in the tricarboxylic acid cycle, such as succinic acid, suggesting that celastrol upregulates mitochondrial respiration in PAH-PASMCS (Online Figure XIIC). Here, we have measured the activities of the enzymes that regulate the levels of succinic acid (succinyl-CoA synthetase and succinate dehydrogenase) in PAH-PASMCS. Interestingly, celastrol significantly increased both enzymes (Online Figure XIIC). However, the extents of the increases were higher for succinyl-CoA synthetase (+140%) than for SDHA (succinate dehydrogenase complex subunit A; +20%; Online Figure XIIC). Thus, the increased levels of succinic acid by celastrol can be explained, at least in part, by the increased ratio of succinyl-CoA synthetase/SDHA. Additionally, we further performed analyses of cytokines/chemokines and growth factors in conditioned medium from control PASMCS and PAH-PASMCS under treatment with celastrol (Online Figure XIID). Importantly, celastrol treatment significantly reduced the secretion of cytokines/chemokines and growth factors from PAH-PASMCS, which were elevated compared with control PASMCS at baseline (Online Figure XIID). These results suggest that celastrol changes the cell metabolism and reduces inflammatory cytokines/chemokines and growth factors in PAH-PASMCS.

Celastrol Inhibits Inflammatory Signaling in PAH-PASMCS

Celastrol was originally identified as a potent suppressor of immune deficiency pathways, which regulate Gram-positive bacterial infections via transcription factor NF- κ B (nuclear factor κ B)-like transcriptional factor.^{11,12} Inflammation and oxidative stress are closely connected by cytokines/chemokines and growth factors.¹⁵ Excessively augmented NF- κ B expression is recognized in PAH-PASMCS and induces the transcription of many genes producing proliferative and proinflammatory signals and impaired mitochondrial metabolism.³⁵ Consistent with this, knockdown of NF- κ B by small interfering RNA (siRNA) significantly reduced PAH-PASC proliferation compared with control siRNA (Figure 4A). Importantly, celastrol treatment significantly reduced protein levels of NF- κ B in the nuclear extracts of PAH-PASMCS compared with vehicle controls (Figure 4B). Moreover, phosphorylation of ERK (extracellular signal-regulated kinases) 1/2 in total cell lysates was significantly upregulated in PAH-PASMCS compared with control PASMCS, which was significantly reduced by celastrol treatment (Figure 4C). Additionally, celastrol significantly reduced gene expression levels of NF- κ B (*RELA*) and Toll-like receptor 4 (*TLR4*) compared with vehicle controls (Figure 4D). These results suggest that celastrol inhibits inflammation through suppression of TLR4-NF- κ B-ERK signaling in PAH-PASMCS. BRD4 (bromodomain-containing

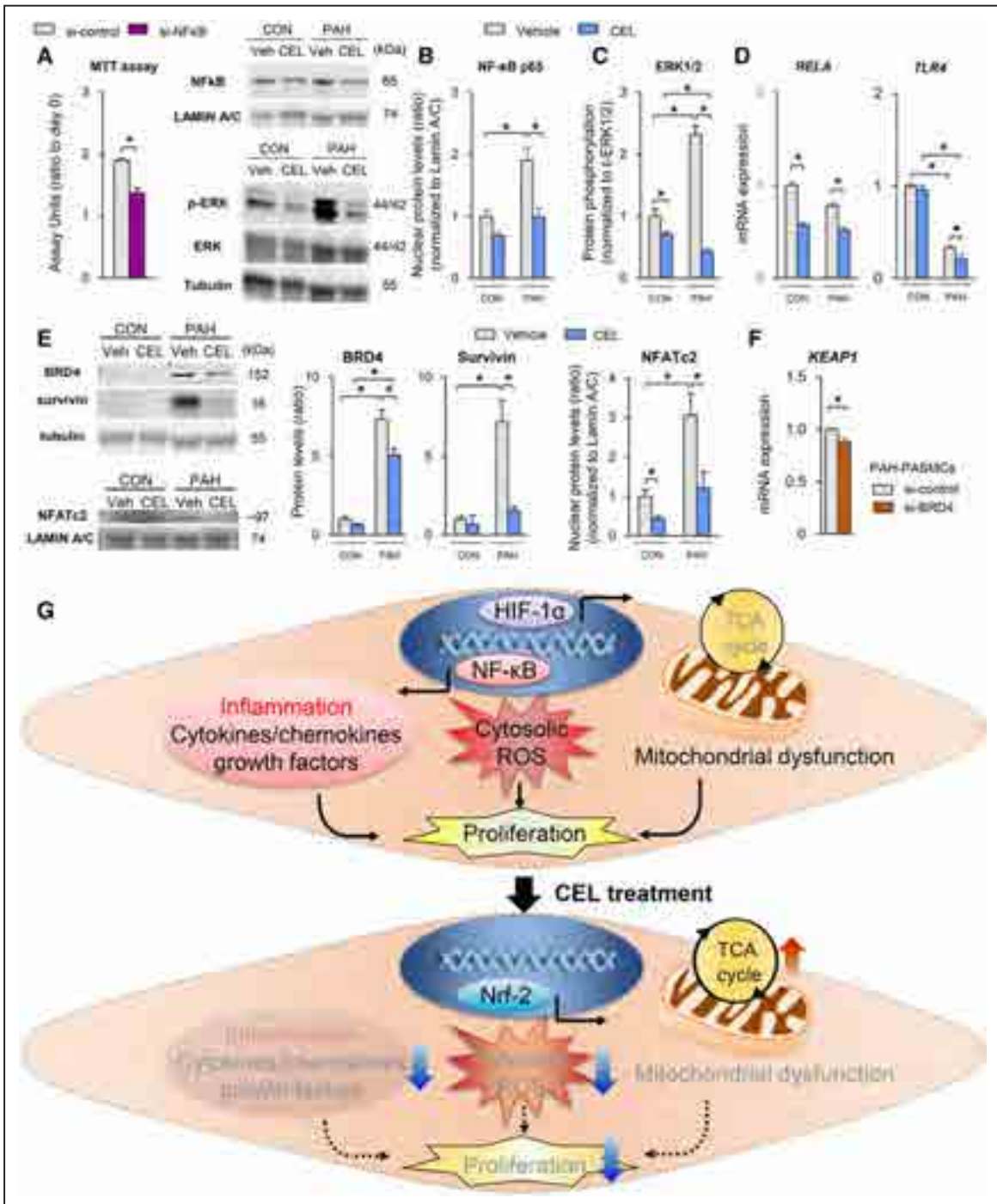


Figure 4. Cellastramycin (CEL)-mediated inhibition of pulmonary artery smooth muscle cells from patients with pulmonary arterial hypertension (PAH-PASMC) proliferation. **A**, The ratio of cell numbers in PAH-PASMCs treated with control small interfering RNA (si-control) or si-NF-κB (nuclear factor κB) for 48 h (n=8 each). Cell numbers were measured by 3-(4,5-di-methylthiazol-2-yl)-2,5-diphenyltetrazolium bromide assay. **B**, Quantification of NF-κB in nuclear extracts of control PASMCs and PAH-PASMCs after the treatment with CEL or the control vehicle for 24 h (n=6). **C**, Quantification of phosphorylated ERK (extracellular signal-regulated kinases)1/2 and total ERK1/2 in total cell lysates of control PASMCs and PAH-PASMCs after the treatment with CEL or the control vehicle for 24 h (n=6). **D**, Real-time polymerase chain reaction (RT-PCR) of NF-κB p65 (*RELA*) and toll-like receptor 4 (*TLR4*) mRNA in control PASMCs and PAH-PASMCs after the treatment with CEL or the control vehicle for 24 h (n=6). **E**, Quantification of BRD4 (bromodomain-containing protein 4) and survivin in total cell lysate and NFATc2 (nuclear factor of activated T cells 2) in nuclear extract of control PASMCs and PAH-PASMCs after the treatment with CEL or vehicle for 24 h (n=6). **F**, RT-PCR analysis of Keap1 (Kelch-like ECH-associated protein 1; *KEAP1*) mRNA in PAH-PASMCs after treatment with si-BRD4 or si-control for 48 h (n=6). **G**, Schematic representation of the molecular mechanisms promoting inflammation, oxidative stress, and mitochondrial dysfunction through activation of HIF-1α (hypoxia-inducible factor 1α) and NF-κB in PAH-PASMCs. Constitutively activated HIF-1α induces the transcription of many genes and dysregulation of mitochondrial energy metabolism, which promotes cell proliferation, apoptosis-resistance, survival, and stress resistance by targeting several downstream genes. CEL treatment downregulates HIF-1α and NF-κB and upregulates Nrf2 (nuclear factor erythroid 2-related factor 2) in PAH-PASMCs. These effects result in decreased reactive oxygen species (ROS) and inflammation with recovered mitochondrial energy metabolism, leading to inhibition of excessive proliferation in PAH-PASMCs. Data represent the mean±SEM. **P*<0.05. Comparisons of parameters were performed with 2-way ANOVA, followed by Tukey honestly significant difference test for multiple comparisons. CON indicates control; TCA, tricarboxylic acid; and Veh, vehicle.

protein 4) is an epigenetic reader that binds to acetylated histone tails and other proteins to regulate transcription of genes involved in many cellular functions, such as cell cycle, apoptosis, and inflammation.³⁶ Here, protein levels of BRD4 in PAH-PASMCs was significantly upregulated compared with control PASMCs, which was significantly reduced by celestramycin treatment (Figure 4E). Additionally, celestramycin treatment significantly reduced protein levels of survivin and translocation of NFATc2 (nuclear factor of activated T cells 2) to the nucleus, both of which are downstream of BRD4 and regulate the cell cycle in PAH-PASMCs (Figure 4E). Here, based on the previous reports,^{37,38} we hypothesized that celestramycin-mediated downregulation of BRD4 may have effects on Keap1-Nrf2 signaling. Indeed, inhibition of BRD4 by siRNA significantly reduced the expression of Keap1 (Figure 4F). Altogether, celestramycin reverses altered mitochondrial metabolism and reduces inflammation and ROS production through changes in HIF-1 α , NF- κ B, and Nrf2, leading to inhibition of excessive proliferation in PAH-PASMCs (Figure 4G). Recently, there is mounting evidence that dysfunctional DNA-damage response mechanisms promote resistance to apoptosis and proliferative phenotype in PAH-PASMCs.³⁹ Interestingly, we found that DNA damage was significantly increased in PAH-PASMCs compared with control PASMCs, both of which were significantly reduced by celestramycin treatment in a dose-dependent manner (Online Figure XIII A). Consistently, protein levels of γ H2AX were significantly reduced by celestramycin treatment (Online Figure XIII B). Indeed, PAH is characterized by elevation of circulating cytokines (eg, IL-6) that promotes DNA damage²² and oxidative stress that induces DNA damage through DNA base oxidation and deamination.³⁹ Thus, celestramycin-mediated anti-inflammatory and antioxidative effects may have alleviated the DNA damage especially in PAH-PASMCs. Next, we further evaluated the enzyme implicated in DNA repair, PARP-1 (poly [ADP-ribose] polymerase-1), in control PASMCs and PAH-PASMCs. However, celestramycin did not have any significant effects on the protein levels of PARP-1 (Online Figure XIII B). Altogether, celestramycin may play as a modulator of DNA damage with anti-inflammatory and antioxidative effects on PAH.

Zinc Finger C3H1 Domain-Containing Protein-Mediated Inhibition of BRD4 and HIF-1 α by Celestramycin Treatment

A recent study clearly demonstrated that ZFC3H1 (zinc finger C3H1 domain-containing protein; encoded by *ZFC3H1*) is a binding partner of celestramycin.¹³ Moreover, ZFC3H1 plays a crucial role in the degradation of nuclear RNAs, such as mRNAs, ribosomal RNAs, and noncoding RNAs and thus regulates multiple intracellular signaling pathways.^{40–42} Here, we hypothesized that celestramycin-mediated inhibitory effects on transcriptional modulators could be regulated by its binding partner, ZFC3H1. Indeed, inhibition of ZFC3H1 by siRNA significantly reduced the mRNA expression and protein levels of BRD4 (Figure 5A). Additionally, inhibition of ZFC3H1 by siRNA significantly reduced the expression of HIF-1 α and its downstream DRP1 (Figure 5B). Moreover, inhibition of ZFC3H1 induced downregulation of Keap1 and

resultant upregulation of Nrf2 and SOD2 (Figure 5C). In contrast, we overexpressed ZFC3H1 in PAH-PASMCs using a ZFC3H1-encoding plasmid. Importantly, overexpression of ZFC3H1 significantly upregulated BRD4, HIF1 α , DRP1, and Keap1 (Figure 5D through 5F). Altogether, celestramycin-mediated multiple effects can be explained by the inhibition of ZFC3H1, leading to suppression of BRD4 and HIF-1 α (Figure 5G). However, celestramycin significantly increased the expression of PGC1 α and its downstream signaling, TFAM, PPARA (peroxisome proliferator-activated receptor- α), and PPARD (peroxisome proliferator-activated receptor- δ) in PAH-PASMCs (Online Figure VIII E), which upregulate the expression of mitofusin 2 and mitochondrial biogenesis.⁴³ Here, we have demonstrated that AMPK (AMP-activated protein kinase) plays a crucial role against the development of PAH.¹⁸ Additionally, AMPK contributes to the activation of PGC1 α and mitochondrial biogenesis,^{44,45} and mROS are a physiological activator of AMPK signaling.⁴⁶ Thus, we consider that celestramycin-mediated upregulation of mROS may have activated AMPK and downstream PGC1 α in PAH-PASMCs. Indeed, celestramycin treatment significantly increased the phosphorylation of AMPK, which increases the expression of PGC1 α , especially in PAH-PASMCs (Online Figure VIII F). Altogether, celestramycin-mediated multiple effects are based on its inhibitory effects on its binding partner, ZFC3H1 (Figure 5G).¹³

Celestramycin Ameliorates PH in Rodent Models

Based on the celestramycin-mediated inhibitory effects on PAH-PASMC proliferation, we performed *in vivo* experiments in rodent models of PH. First, we examined the effect of celestramycin in hypoxia-induced PH in mice (Figure 6A). Daily administration of celestramycin using osmotic pumps during 21 days of normoxia or chronic hypoxia had no effect on body weight or blood pressure compared with vehicle controls (Figure 6B and 6C). Moreover, celestramycin treatment significantly reduced cytokines/chemokines and growth factors in the lungs, many of which were significantly increased under hypoxia compared with normoxic controls (Figure 6D, Online Table III). Importantly, celestramycin significantly reduced perivascular inflammation (Online Figure XIV) and muscularization of distal pulmonary arteries (Figure 6E) after hypoxic exposure compared with vehicle controls. Consistently, celestramycin significantly ameliorated hypoxia-induced increases in RVSP (RV systolic pressure) and RV hypertrophy compared with vehicle controls (Figure 6F). Next, to further assess the therapeutic potential of celestramycin for PAH, we used a model of monocrotaline-induced PH in rats (Figure 7A). In this monocrotaline-induced rat model, we started celestramycin treatment during the development of PH (prevention protocol). Daily administration of celestramycin for 3 weeks had no effect on body weight or food consumption compared with vehicle controls (Figure 7B). Again, consistent with the results *in vitro*, celestramycin treatment significantly reduced cytokines/chemokines and growth factors in the lung compared with vehicle controls (Figure 7C, Online Table III). Moreover, celestramycin significantly suppressed muscularization of distal pulmonary arteries compared with vehicle controls (Figure 7D). Consistently, celestramycin treatment

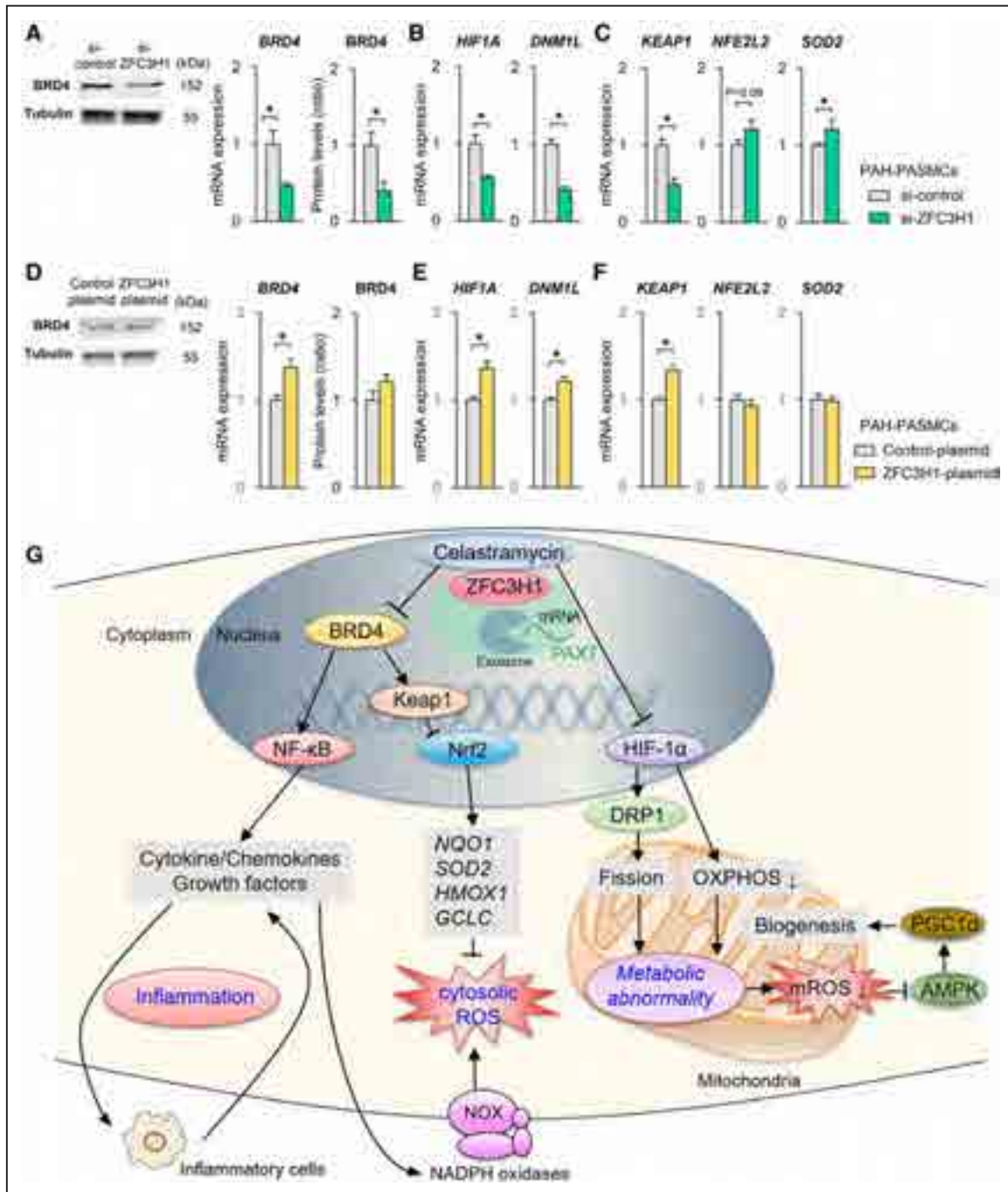


Figure 5. ZFC3H1 (zinc finger C3H1 domain-containing protein)-mediated inhibition of BRD4 (bromodomain-containing protein 4) and HIF-1 α (hypoxia-inducible factor 1 α) by celastramycin treatment. **A**, Real-time polymerase chain reaction (RT-PCR) analysis and Western blotting of BRD4 in pulmonary artery smooth muscle cells from patients with pulmonary arterial hypertension (PAH-PASMCs) after treatment with si-ZFC3H1 or si-control for 48 h (n=6). **B**, RT-PCR analysis of HIF-1 α (*HIF1A*) and dynamin-1-like protein (*DNMT1*) mRNA in PAH-PASMCs after treatment with si-ZFC3H1 or si-control for 48 h (n=6). **C**, RT-PCR analysis of Keap1 (Kelch-like ECH-associated protein 1; *KEAP1*), Nrf2 (nuclear factor erythroid 2-related factor 2; *NFE2L2*), and SOD2 (superoxide dismutase 2; *SOD2*) mRNA in PAH-PASMCs after treatment with si-ZFC3H1 or si-control for 48 h (n=6). **D**, RT-PCR analysis and Western blotting of BRD4 in PAH-PASMCs after the treatment with *ZFC3H1* plasmid DNA or control plasmid DNA for 48 h (n=6). **E**, RT-PCR analysis of HIF-1 α (*HIF1A*) and dynamin-1-like protein (*DNMT1*) mRNA in PAH-PASMCs after the treatment with *ZFC3H1* plasmid DNA or control plasmid DNA for 48 h (n=6). **F**, RT-PCR analysis of Keap1 (*KEAP1*), Nrf2 (*NFE2L2*), and SOD2 (*SOD2*) mRNA in PAH-PASMCs after the treatment with *ZFC3H1* plasmid DNA or control plasmid DNA for 48 h (n=6). **G**, Schematic representation of the molecular mechanisms of celastramycin-mediated effects on PAH-PASMCs. Abnormally activated HIF-1 α and NF- κ B (nuclear factor- κ B) promotes inflammation, oxidative stress, and mitochondrial dysfunction, which induce excessive proliferation of PAH-PASMCs. Activation of NF- κ B also increases production of cytokines/chemokines and growth factors, which recruit abundant inflammatory cells, leading to additional production of growth factors. Secreted growth factors activate NOX (NADPH oxidases), one of the main sources of intracellular reactive oxygen species (ROS), and induce production of cytosolic ROS in PAH-PASMCs. Here, celastramycin directly binds to ZFC3H1, a zinc finger protein, which downregulates the expression of BRD4 and HIF-1 α . Celastramycin-mediated decrease in BRD4 downregulates NF- κ B and Keap1, which suppress inflammation and activate Nrf2, leading to upregulation of antioxidants, such as NAD(P)H quinone dehydrogenase-1 (*NQO1*), superoxide dismutase 2 (*SOD2*), heme oxygenase-1 (*HMOX1*), and glutamate-cysteine ligase catalytic subunit (*GCLC*), resulting in inhibition of ROS production. Constitutively activated HIF-1 α in PAH-PASMCs upregulates DRP1 (dynamin-1-like protein) and promotes mitochondrial fission and induces dysregulation of mitochondrial energy metabolism, (*Continued*)

Figure 5 Continued. leading to less oxidative phosphorylation (OXPHOS) with metabolic abnormality. Mitochondrial ROS (mROS) promotes phosphorylation of AMPK (AMP-activated protein kinase) that induces PGC-1 α (peroxisome proliferator-activated receptor γ coactivator 1- α) to promote mitochondrial biogenesis, whereas mROS is downregulated because of mitochondrial metabolic abnormality in PAH-PASMCs. These mitochondrial abnormalities are reversed by ZFC3H1-mediated HIF-1 α downregulation. Altogether, celestramycin inhibited abnormal proliferation of PAH-PASMCs through changes in these transcription factors. Data represent the mean \pm SEM. * P <0.05. Comparisons of parameters were performed with an unpaired Student t test. PAXT indicates poly(A) tail exosome targeting connection; and Si, small interfering.

significantly reduced RVSP and RV hypertrophy compared with vehicle controls (Figure 7E). Finally, to further evaluate the therapeutic potential of celestramycin for PAH, we used a third animal model of PH, in which rats were exposed to chronic hypoxia for 21 days in combination with injection of SU5416 (Sugen/hypoxia model; Figure 8A). In this Sugen/hypoxia rat model, we started celestramycin treatment after the development of PH (treatment protocol). Daily administration of celestramycin for 14 days had no effect on body weight or food consumption compared with vehicle controls (Figure 8B). Protein levels of inflammatory cytokines (eg, IL-2, IL-6) in the lungs were significantly reduced by celestramycin treatment in the Sugen/hypoxia rat model (Figure 8C, Online Figure XV, Online Table III). Moreover, celestramycin significantly suppressed muscularization of distal pulmonary arteries compared with vehicle controls (Figure 8D). Additionally, celestramycin treatment was associated with a marked reduction in proliferation and a trend for increased apoptosis in the distal pulmonary arteries in rats (Online Figure XVI). Consistently, celestramycin treatment significantly reduced RVSP and RV hypertrophy compared with vehicle controls (Figure 8E). Importantly, celestramycin treatment significantly improved hemodynamic parameters, such as RV diastolic diameter, RV fractional area change, pulmonary artery acceleration time, tricuspid annular plane systolic excursion, and cardiac output as determined by echocardiography (Figure 8F). In contrast, celestramycin treatment did not change left ventricular diastolic diameter or left ventricular ejection fraction (Figure 8G). Again, we used a Seahorse XF24-3 apparatus to evaluate the mitochondrial function in cardiomyocytes using neonatal rat cardiomyocytes (Online Figure XVII A). Importantly, we observed higher levels of ATP production, maximal respiration, and OCR/ECAR ratio in celestramycin-treated neonatal rat cardiomyocytes compared with vehicle controls in vitro (Online Figure XVII B and XVII C). Moreover, celestramycin increased the expressions of genes for mitochondrial fusion, such as *MFN1* and *MFN2*, reduced the expressions for mitochondrial fission, such as *FIS1* and mitochondrial fission 2 protein (*Mff*), and upregulated the expressions of genes for mitochondrial biogenesis, such as *TFAM* in neonatal rat cardiomyocytes, compared with vehicle controls (Online Figure XVII D). Here, the metabolic status of neonatal rat cardiomyocytes shifted from aerobic to energetic by the OCR/ECAR analysis (Online Figure XVII C). Indeed, celestramycin treatment significantly reduced mean pulmonary arterial pressure and increased cardiac output (CO), resulting in the significant reduction on total pulmonary vascular resistance compared with vehicle controls (Figure 8H). Altogether, celestramycin treatment significantly improved exercise capacity and increased treadmill walking distance (Figure 8I). These results suggest that celestramycin suppresses inflammation in the lungs and improves systemic metabolism, ameliorating PH and RV failure in several different animal models. Finally, we performed biochemical tests in Sugen/hypoxia-induced PH

model in rats after the treatment with celestramycin or vehicle. Importantly, there was no significant change in the functions of liver and kidney and hematology profiles after the celestramycin treatment (Online Table IV).

Discussion

In this study, we demonstrated that celestramycin inhibits PAH-PASMC proliferation by the suppression of inflammation and oxidative stress and ameliorates PH in 3 different animal models. These concepts are based on the following findings: (1) we selected celestramycin as a compound that inhibits cell proliferation dose-dependently with small effects on control PASMCs, (2) celestramycin treatment increased genes for mitochondrial biogenesis and function, leading to improved mitochondrial energy metabolism and networks, (3) celestramycin significantly diminished nuclear translocation of HIF1- α and NF- κ B and reduced cytokines/chemokines and growth factors, and (4) celestramycin inhibited PASMC proliferation and ameliorated PH in different animal models.

Identification of Celestramycin as a Novel Drug for PAH

There are 3 main types of drugs for treating PAH, all of which aim to dilate the pulmonary arteries.³ However, these treatments cannot stop or reverse this aggressive disease, although they help to slow its progression. Thus, patients with advanced PAH and RV failure require lung transplantation, and some patients die even after the vasodilator therapy with these drugs.⁴ As an additional strategy for PAH, effective treatment that achieves reverse remodeling of pulmonary arteries is warranted. Thus, we focused on the inhibition of PAH-PASMC proliferation to discover a novel drug for PAH. PAH-PASMCs have special characteristics in terms of proproliferative and antiapoptotic features in common with cancer cells.⁶ The development of academic drug discovery is in response to the fact that the discovery of new drugs has come to a standstill in the pharmaceutical industry. Under these situations, the DDI was founded in Japan to promote an environment in which academic drug discovery can be performed. Using these platforms, we were able to promote drug discovery based on a clinical perspective and the knowledge of the pathogenesis of PAH. When we consider the pathological findings of PAH, actively proliferative cell components, and occlusion of the distal pulmonary arteries, it is evident that treatment with pulmonary vasodilators is useful only in patients with mild progression. In the present study, we performed phenotypic screening and discovered compounds with antiproliferative effects on PAH-PASMCs and selected the compounds specific for the cells responsible for the disease. Then, we developed 25 analogs of the hit compound to determine the lead compound and finally selected celestramycin b with antioxidant effects for in vivo treatment. Finally, celestramycin was effective in 3 animal models of PH with no apparent side effects.

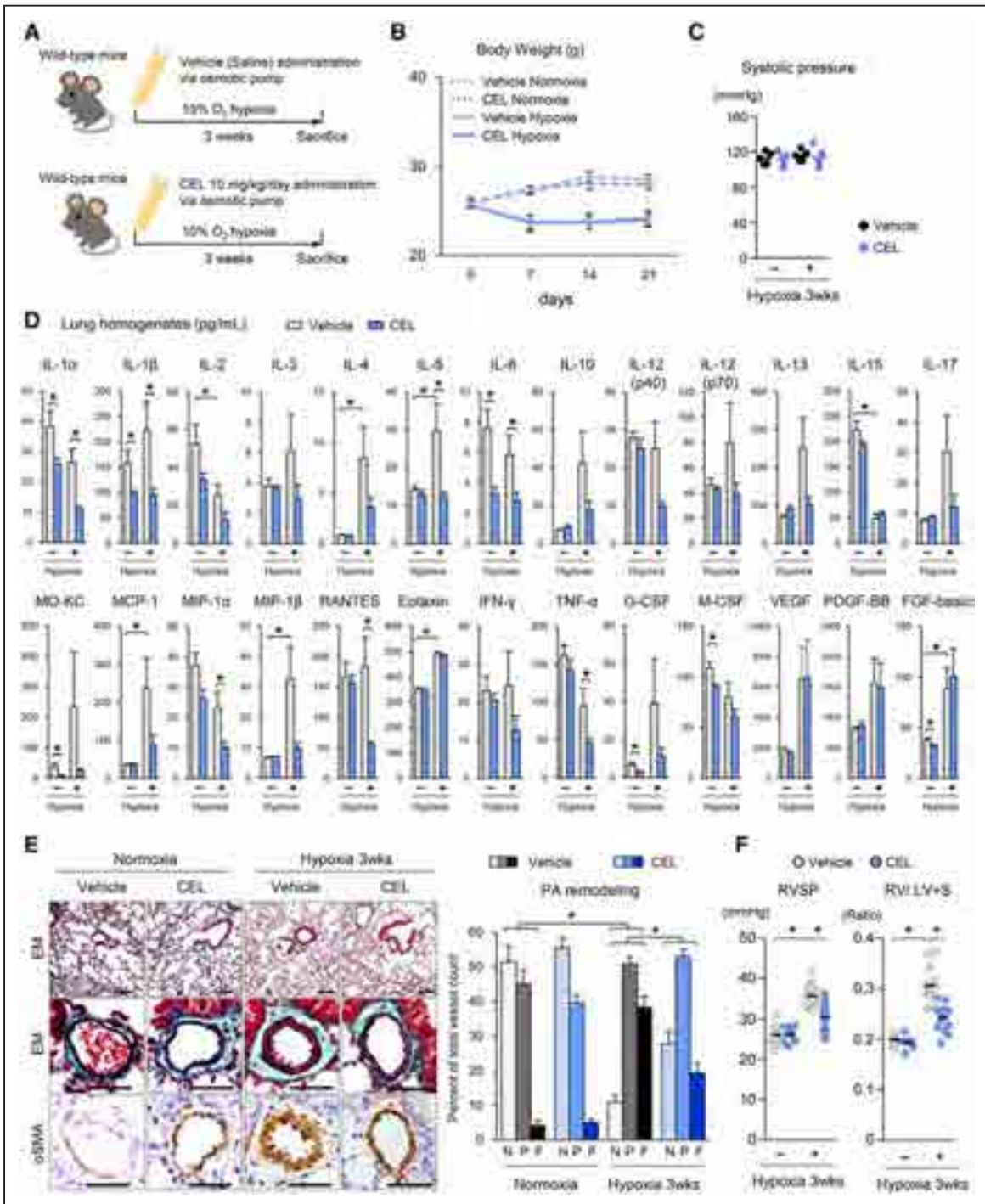


Figure 6. Cellastramycin (CEL) ameliorates hypoxia-induced pulmonary hypertension (PH) in mice. **A**, Schematic protocols for CEL administration to hypoxia-induced PH in wild-type mice, in which 10 mg/(kg·d) CEL or control vehicle was administered using an osmotic pump during the 3 wk of hypoxic exposure (10% O₂). **B**, The time-course of body weight from the starting point of administration of CEL or control vehicle under normoxia (21% O₂, n=8 each) or hypoxia (10% O₂, n=14 each) for 3 wk. **C**, Systolic blood pressure of hypoxia-induced PH mice and control mice measured by tail-cuff systems after the treatment with CEL or control vehicle for 3 wk (n=6 each). **D**, Levels of cytokines/chemokines and growth factors in the lungs after the treatment with CEL or vehicle under normoxia or hypoxia (10% O₂) for 3 wk (n=6 each). **E**, Muscularization of the distal pulmonary arteries (PA) with a diameter of 20–70 μ m after the treatment with CEL or control vehicle under normoxia (n=8 each) or hypoxia (n=14 each). Scale bar, 25 μ m. **F**, Right ventricular systolic pressure (RVSP) and right ventricular hypertrophy (RVH) in wild-type mice after the treatment with CEL or control vehicle under normoxia (n=8 each) or hypoxia (10% O₂, n=14 each) for 3 wk. RVH denotes the ratio of the right ventricle to the left ventricle plus septum (RV/LV+S). Data represent the mean \pm SEM. **P*<0.05. Comparisons of means between 2 groups by the bootstrap method. The multiplicity of the testing was adjusted by the Holm method. α SMA indicates α smooth muscle actin; EM, Elastica-Masson; F, fully muscularized vessels; FGF, fibroblast growth factor; G-CSF, granulocyte-colony stimulating factor; IFN γ , interferon γ ; MCP, monocyte chemotactic protein; M-CSF, macrophage colony-stimulating factor; MIP, macrophage inflammatory protein; MO-KC, mouse keratinocyte-derived chemokine; N, nonmuscularized vessels; P, partially muscularized vessels; PDGF-BB, platelet derived growth factor; RANTES, regulated on activation, normal T cell expressed and secreted; TNF, tumor necrosis factor; and VEGF, vascular endothelial growth factor.

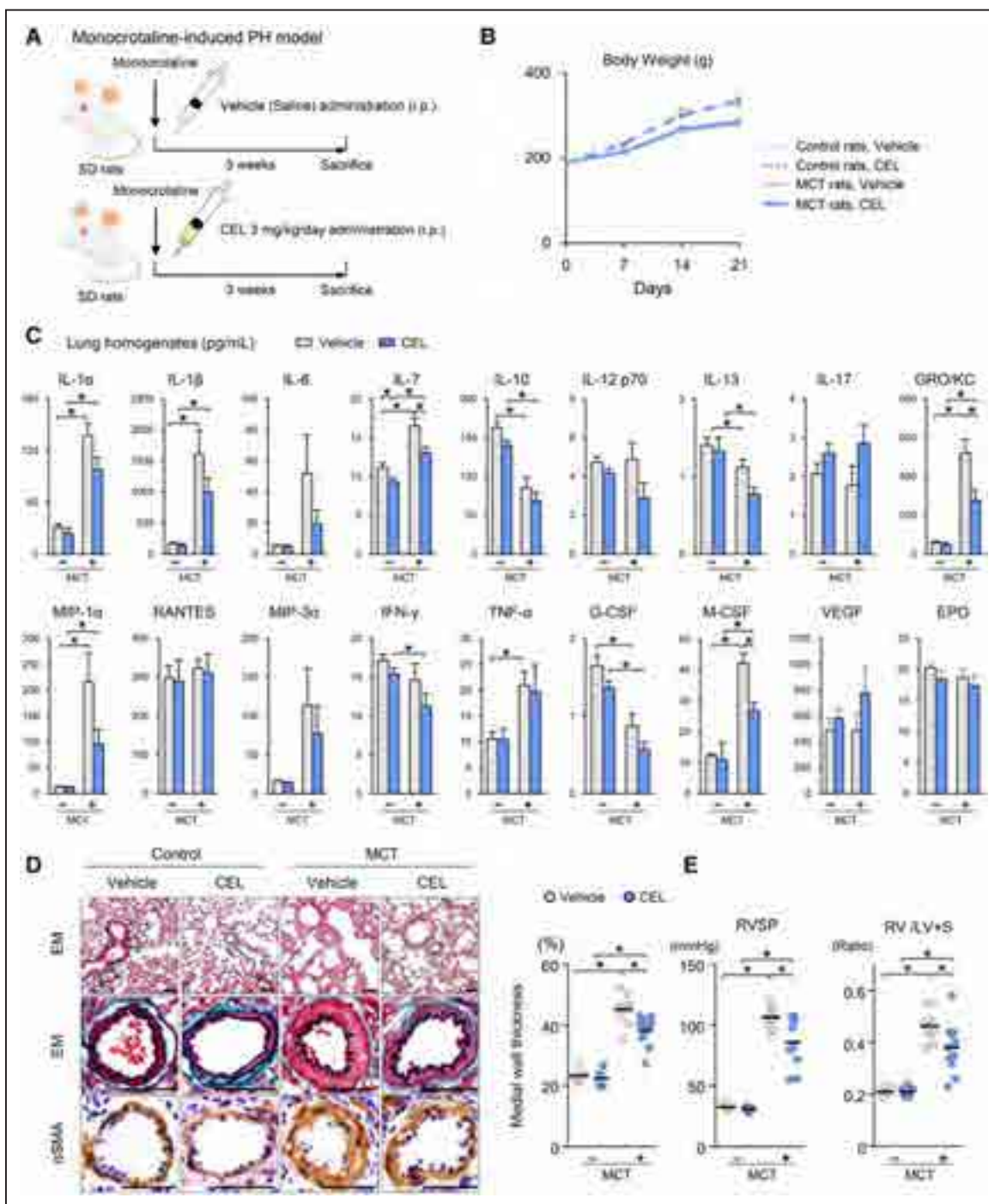


Figure 7. Celastramycin (CEL) ameliorates monocrotaline (MCT)-induced pulmonary hypertension (PH) in rats. **A**, Schematic protocols for CEL administration to MCT-induced PH in rats, in which 3 mg/(kg·d) CEL was administered (intraperitoneal injection) for 3 wk after MCT injection (60 mg/kg, subcutaneous injection). **B**, The time-course of body weight changes from the starting point of administration of CEL or control vehicle for 3 wk ($n=14$). **C**, Levels of cytokines/chemokines and growth factors in the lungs of monocrotaline-induced pulmonary hypertension in rats and control rats after the treatment with CEL or control vehicle for 3 wk ($n=6$ each). **D**, Medial wall thickness of the distal pulmonary arteries in rats (control, $n=7$; CEL and vehicle, $n=11$ each). Scale bar, 50 μm . **E**, Right ventricular (RV) systolic pressure (RVSP, left) and RV hypertrophy (RVH) in rats (control, $n=7$; CEL and vehicle, $n=11$ each). RVH denotes the ratio of the RV to the left ventricle plus septum (RV/LV+S). Data represent the mean \pm SEM. * $P<0.05$. Comparisons of means between 2 groups by the bootstrap method. The multiplicity of the testing was adjusted by the Holm method. α SMA indicates alpha smooth muscle actin; EM, Elastica-Masson; EPO, erythropoietin; G-CSF, granulocyte-colony stimulating factor; GRO/KC, growth-related oncogene/keratinocyte-derived chemokines; IFN γ , interferon γ ; IL, interleukin; M-CSF, macrophage colony-stimulating factor; MIP, macrophage inflammatory protein; RANTES, regulated on activation, normal T cell expressed and secreted; TNF, tumor necrosis factor; and VEGF, vascular endothelial growth factor.

This means that the antiproliferative strategy for PASMCs may be a novel therapeutic strategy to treat patients with PAH; celastramycin can be a possible drug for PAH. In the

previous article, we have already discovered sanguinarine that reduces selenoprotein P expression and PASMC proliferation and ameliorates PH in mice and rats.^{19,47,48} In the present study,

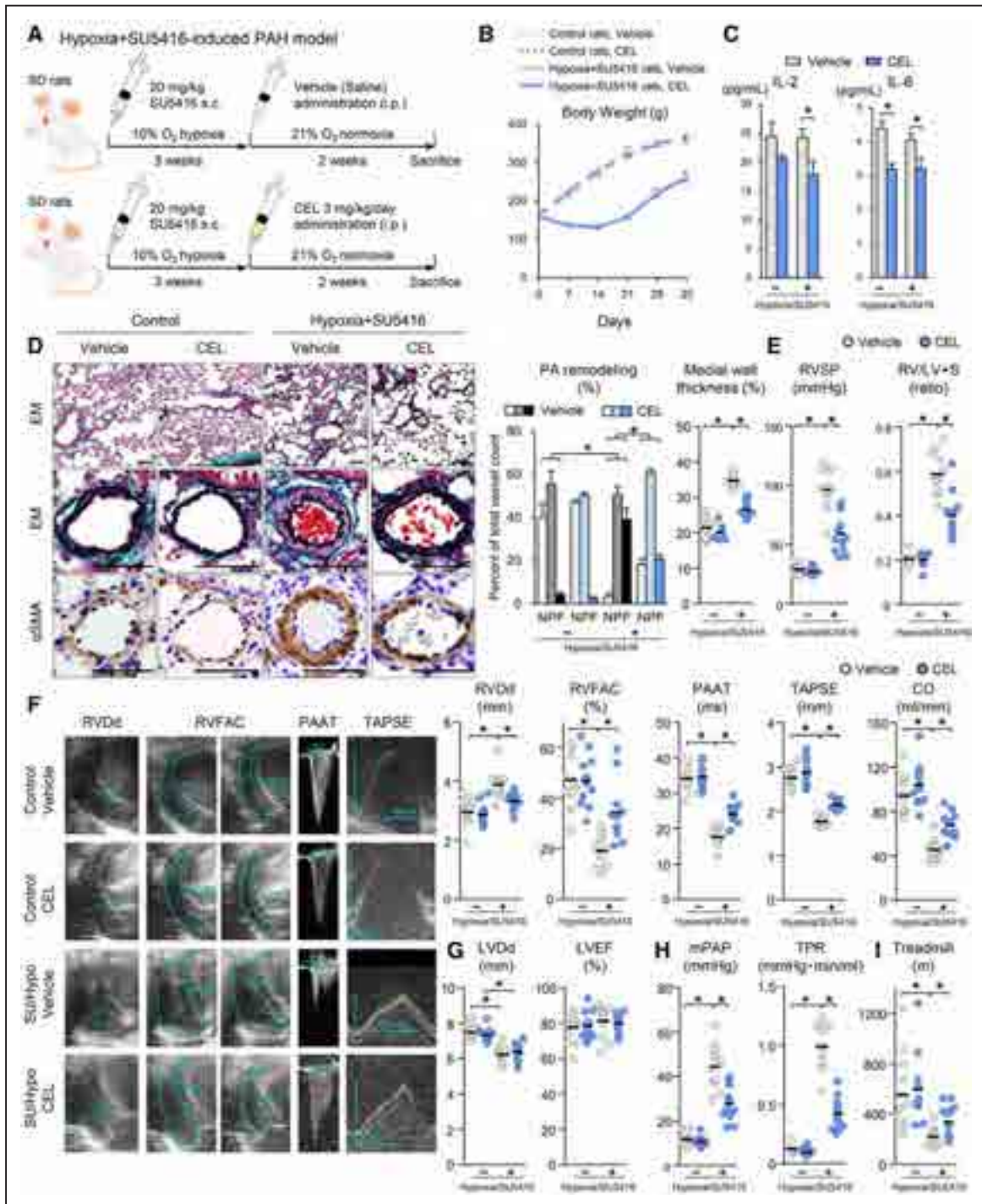


Figure 8. Celastramycin (CEL) ameliorates sugen/hypoxia-induced pulmonary hypertension in rats. **A**, Schematic protocols for CEL administration to the Sugén/hypoxia rat model, in which rats were exposed to chronic hypoxia (10% O₂) for 3 wk in combination with the VEGF (vascular endothelial growth factor) receptor blocker SU5416 (20 mg/kg, subcutaneous injection) followed by daily administration of 3 mg/kg body weight CEL or control vehicle by intraperitoneal injection for 2 wk. **B**, The time-course of body weight changes from the starting point of SU5416 injection for 5 wk in Sugén/hypoxia rats and control rats (n=12 each). **C**, Levels of IL (interleukin)-2 and IL-6 in the lungs of Sugén/hypoxia rats and control rats after the treatment with CEL or control vehicle for 2 wk (n=6 each). **D**, **Left**, Representative pictures of distal pulmonary arteries (PAs). **Middle**, muscularization of the distal PAs with a diameter of 50–100 μm after the treatment with CEL or vehicle control in rats (n=12 each). **Right**, medial wall thickness of the distal PAs in rats (n=12 each). Scale bar, 50 μm. **E**, Right ventricular (RV) systolic pressure (RVSP) and RV hypertrophy (RVH; n=12 each). RVH denotes the ratio of the RV to the left ventricle plus septum (RV/LV+S). **F**, **Left**, Representative echocardiographic images illustrating RV diastolic diameter (RVDd), RV fractional area change (RVFAC), PA acceleration time (PAAT), and tricuspid annular plane systolic excursion (TAPSE). **Right**, Echocardiographic measurement of RVDd, RVFAC, PAAT, TAPSE, and cardiac output (CO; n=12 each). **G**, Echocardiographic measurement of LV diastolic diameter (LVDd) and LV ejection fraction (LVEF; n=12 each). **H**, Mean PAs pressure (mPAP) and total pulmonary resistance (TPR) in rats (n=12 each). **I**, Walking distance assessed by treadmill test (n=12 each). Data represent the mean±SEM. *P<0.05. Comparisons of means between 2 groups by the bootstrap method. The multiplicity of the testing was adjusted by the Holm method. αSMA indicates alpha smooth muscle actin; EM, Elastica-Masson; F, fully muscularized vessels; N, nonmuscularized vessels; P, partially muscularized vessels; and PAH, pulmonary arterial hypertension.

we used our different original library and selected celastramycin by rigorous screening to verify its safety on normal cells, which implies that celastramycin has different effects on PAH-PASMCs compared with the effects of sanguinarine-mediated inhibition of selenoprotein P.

ZFC3H1-Mediated Anti-Inflammatory Effects by Celastramycin

In the present study, celastramycin inhibited NF- κ B nuclear translocation and exerted anti-inflammatory effects on PAH-PASMCs in vitro and in rodent models of PH in vivo. Celastramycin is a benzoyl pyrrole-type compound originally discovered as a new antibiotic in the extract of *Streptomyces* MaB-QuH-8 from the plants of the Celastraceae in 2002.⁴⁹ Then, after searching for natural substances that regulate innate immunity using an ex vivo *Drosophila* culture system, celastramycin was identified as a potent suppressor of immune deficiency pathways, which regulate Gram-positive bacterial infections via transcription factor NF- κ B-like transcriptional factor.^{11,12} Thus, NF- κ B-related signal transduction pathways seem to be a target for celastramycin in mammalian cells.¹³ Inflammatory cytokines, such as IL-1 β , IL-6, and TNF- α , are involved in NF- κ B signaling and play crucial roles in the development of PAH.^{50–52} Thus, the anti-inflammatory effect of celastramycin is one of its main mechanisms of action. A recent study identified that ZFC3H1, an uncharacterized zinc finger protein, is a binding partner of celastramycin, which blocks the formation of the NF- κ B transcription complex.¹³ Moreover, ZFC3H1 links ATP-dependent RNA helicase MTR4 with polyadenylate-binding nuclear protein 1 in the poly(A) tail exosome targeting connection, which plays a crucial role in the degradation of nuclear RNAs.^{40,41} Exosomes are involved in the processing of a wide range of RNAs, including mRNAs, ribosomal RNAs, and noncoding RNAs,⁴² and have been shown to regulate the production of cytokines and other inflammatory proteins.⁵³ Thus, celastramycin may modulate poly(A) tail exosome targeting connections by binding to ZFC3H1, resulting in changes in the degradation of RNAs with inflammatory effects. Indeed, celastramycin-mediated multiple effects were due to the inhibition of ZFC3H1, leading to suppression of BRD4 and HIF-1 α .

Celastramycin Reduces Cytosolic ROS in PAH-PASMCs

There is mounting evidence of the role of oxidative stress in the pathogenesis of PAH.¹⁵ In the present study, celastramycin significantly reduced cytosolic ROS in PAH-PASMCs. A possible mechanism of this celastramycin-mediated reduced cytosolic ROS is the upregulation of Nrf2, which is essential for oxidative and electrophilic stress responses, and resultant downregulation of NADPH oxidase activities.^{30,31} Here, it has been demonstrated that NADPH oxidase regulates the activities of Nrf2 in several cell lines.^{30,31} Conversely, Keap1-Nrf2 pathway regulates the cytosolic ROS production through inhibition of NADPH oxidases.³² Indeed, celastramycin treatment significantly reduced NADPH oxidase activity and Keap1 and upregulated downstream Nrf2 in PAH-PASMCs. Induction of the Nrf2 transcript is an effective approach for enhancing the activity of Nrf2, although Nrf2 activity is tightly regulated by

proteasomal degradation via Keap1-mediated ubiquitination.⁵⁴ Nrf2 enables adaptation to oxidants and electrophiles by stimulating the transcriptional activation of about 100 cytoprotective genes, including *GCLC*, which regulates glutathione biosynthesis, *HMOX1*, which catalytically degrades potentially toxic heme to biliverdin, and *NQO1*, which inhibits the formation of free radicals via the redox-cycling of quinones. Indeed, in the present study, celastramycin significantly upregulated mRNA levels of *GCLC*, *HMOX1*, and *NQO1* and protein levels of GSH in PAH-PASMCs. Consistently, activation of Nrf2 inhibited PASC proliferation and ameliorated hypoxia-induced PH in mice.⁵⁵ In contrast, celastramycin treatment significantly increased mROS in PAH-PASMCs. This is consistent with the higher levels of ATP production, maximal respiration, and OCR/ECAR ratio in celastramycin-treated cells. Dysregulated mitochondria in PAH-PASMCs show lower mROS production compared with normal PASMCs, and an increase in mROS causes apoptosis in PAH-PASMCs.^{56–58} These data indicate that the celastramycin-mediated reduction in ROS (eg, Nrf2-mediated ROS scavengers, NADPH oxidase-derived ROS reduction) was significant as compared to the celastramycin-mediated increase in mitochondrial ROS production. In total, celastramycin reduced the levels of cytosolic ROS (assessed by 2,7-dichlorodihydrofluorescein and CellROX) through significant upregulation of Nrf2 (ROS scavengers), downregulation of NADPH oxidases, and slight increase in mitochondrial ROS (by increased mitochondrial respiration and ATP production) in PAH-PASMCs.

Celastramycin Improves Mitochondrial Metabolism and Networks in PAH-PASMCs

Celastramycin treatment increased OCR and OCR/ECAR ratio in PAH-PASMCs. The reason why the tricarboxylic acid cycle is upregulated may be that celastramycin reduces PDK1, which inactivates PDH to convert pyruvic acid to acetyl CoA. Additionally, celastramycin treatment ameliorated mitochondrial morphology. The mitochondrial network is fragmented in PAH-PASMCs,²⁹ and this disruption is mechanistically related to imbalanced proliferation and apoptosis in PAH-PASMCs.²⁹ Fragmentation of the mitochondrial network reflects, in part, increased fission.⁴³ Fission creates smaller, more discrete mitochondria, which facilitates mitophagy, or accelerates cell proliferation.⁵⁹ When mitochondria cannot divide, mitosis does not proceed, and cells are arrested in the G2-M phase of the cell cycle.⁷ Thus, it is conceivable that celastramycin normalized the balance between fission and fusion in PAH-PASMCs, resulting in increased mitochondrial network activity and decreased proliferation. A possible mechanism of the celastramycin-mediated alteration in this balance may be the downregulation of HIF-1 α , which is excessively activated in PAH-PASMCs and is likely an upstream stimulus for impaired mitochondrial fusion and enhanced fission in PAH.²⁹ Indeed, celastramycin treatment reduced the levels of DRP1, which promotes mitochondrial fission, in PAH-PASMCs. The reason for the celastramycin-mediated downregulation of HIF-1 α may involve the suppression of NF- κ B signaling. Indeed, NF- κ B has been shown to directly affect HIF-1 α expression at the HIF-1 α promoter region, contributing to the regulation of basal levels of mRNA and protein. Additionally, NF- κ B-mediated

downstream inflammatory cytokines also have direct effects on mitochondrial function in PAH-PASMCs.^{9,16} Furthermore, celastramycin-mediated upregulation of *HMOX1* should lead to altered mitochondrial energy metabolism. Indeed, it has been reported that *HMOX1* in the heart stimulates mitochondrial biogenesis via the induction of Nrf2 and its nuclear translocation. The number of mitochondria is regulated by mitochondrial biogenesis to meet the energy demands of the cell and compensate for cell damage.⁵⁹ Thus, celastramycin may have altered the mitochondrial energy metabolism through the progression of mitochondrial biogenesis in PAH-PASMCs. Finally, celastramycin-mediated functional improvement of exercise capacity in the Sugen/hypoxia model indicated that celastramycin directly affects cardiac myocytes in addition to PASMCs in terms of mitochondrial biogenesis. We consider that the celastramycin-mediated metabolic changes may have contributed to the greater effects in Sugen/hypoxia-induced model rather than monocrotaline-induced model.

Study Limitations

There are several limitations to the present study. First, we mainly evaluated ROS levels (cytosolic and mitochondrial), inflammation, and mitochondrial energy metabolism, but there might be other mechanisms through which celastramycin suppresses cell proliferation. Indeed, celastramycin treatment significantly upregulated the eNOS levels, which increase NO production in PAECs. Nrf2 activators are in clinical trial for PH treatment and Nrf2 activation can increase NO and decrease superoxide generation.⁶⁰ Thus, it is possible that the mechanism of action of celastramycin is actually via Nrf2-dependent NO upregulation, which could explain both the decreased RVSP and RV hypertrophy (both via direct effects of NO in cardiomyocytes and also in response to reduced RVSP) rather than an entirely PASMC-mediated effect. Moreover, new approaches for PAH therapy need to show benefit on the top of optimized treatment with currently approved therapy.²⁰ Thus, the combination of celastramycin with other drugs, such as sildenafil, should be examined in the future. Second, the cytokine data in 3 animal models are complex and difficult to clearly understand because of the different models with different mechanisms. Third, we were unable to use cardiomyocytes from patients with PAH because it is difficult for us to perform primary culture of cardiomyocytes from patients with PAH.⁹ Finally, we selected celastramycin from the 25 analogs, but other analog might have better effects in vivo because some other analogs inhibited cell proliferation more strongly than celastramycin in vitro.

Clinical Implications and Conclusions

We found that celastramycin inhibits proliferation of PAH-PASMCs in a dose-dependent manner with small effect on control PASMCs via anti-inflammatory and antioxidant effects, accompanied by metabolic improvement. Consistently, celastramycin successfully ameliorated hypoxia-induced PH in mice, monocrotaline-induced PH in rats, and Sugen/hypoxia-induced PH in rats. In conclusion, we discovered a new antiproliferative compound, celastramycin, which is effective in rodent models of PH. Celastramycin could be a promising drug for the treatment of patients with PAH.

Acknowledgments

We are grateful to the lab members in the Department of Cardiovascular Medicine at Tohoku University for valuable technical assistance, especially Yumi Watanabe, Ai Nishihara, and Hiromi Yamashita and the assistants of gas chromatography-mass spectrometry analyses at Tohoku Medical Megabank Organization, especially Reina Saijo and Keiko Umeda.

Sources of Funding

This work was supported in part by the grants-in-aid for Scientific Research (15H02535, 15H04816 and 15K15046), all of which are from the Ministry of Education, Culture, Sports, Science and Technology, Tokyo, Japan; the grants-in-aid for Scientific Research from the Ministry of Health, Labour, and Welfare, Tokyo, Japan (10102895); and the grants-in-aid for Scientific Research from the Japan Agency for Medical Research and Development, Tokyo, Japan (15ak0101035h0001, 16ek0109176h0001, 17ek0109227h0001).

Disclosures

None.

References

- Ryan JJ, Archer SL. Emerging concepts in the molecular basis of pulmonary arterial hypertension: part I: metabolic plasticity and mitochondrial dynamics in the pulmonary circulation and right ventricle in pulmonary arterial hypertension. *Circulation*. 2015;131:1691–1702. doi: 10.1161/CIRCULATIONAHA.114.006979
- Michelakis ED. Pulmonary arterial hypertension: yesterday, today, tomorrow. *Circ Res*. 2014;115:109–114. doi: 10.1161/CIRCRESAHA.115.301132.
- Lai YC, Potoka KC, Champion HC, Mora AL, Gladwin MT. Pulmonary arterial hypertension: the clinical syndrome. *Circ Res*. 2014;115:115–130. doi: 10.1161/CIRCRESAHA.115.301146
- Montani D, Chamaus MC, Guignabert C, Günther S, Girerd B, Jaïs X, Algalarrondo V, Price LC, Savale L, Sitbon O, Simonneau G, Humbert M. Targeted therapies in pulmonary arterial hypertension. *Pharmacol Ther*. 2014;141:172–191. doi: 10.1016/j.pharmthera.2013.10.002
- Humbert M, Sitbon O, Chaouat A, et al. Survival in patients with idiopathic, familial, and anorexigen-associated pulmonary arterial hypertension in the modern management era. *Circulation*. 2010;122:156–163. doi: 10.1161/CIRCULATIONAHA.109.911818
- Abe K, Toba M, Alzoubi A, Ito M, Fagan KA, Cool CD, Voelkel NF, McMurtry IF, Oka M. Formation of plexiform lesions in experimental severe pulmonary arterial hypertension. *Circulation*. 2010;121:2747–2754. doi: 10.1161/CIRCULATIONAHA.109.927681
- Marsboom G, Toth PT, Ryan JJ, Hong Z, Wu X, Fang YH, Thenappan T, Piao L, Zhang HJ, Pogoriler J, Chen Y, Morrow E, Weir EK, Rehman J, Archer SL. Dynamin-related protein 1-mediated mitochondrial mitotic fission permits hyperproliferation of vascular smooth muscle cells and offers a novel therapeutic target in pulmonary hypertension. *Circ Res*. 2012;110:1484–1497. doi: 10.1161/CIRCRESAHA.111.263848
- Bonnet S, Rochefort G, Sutendra G, Archer SL, Haromy A, Webster L, Hashimoto K, Bonnet SN, Michelakis ED. The nuclear factor of activated T cells in pulmonary arterial hypertension can be therapeutically targeted. *Proc Natl Acad Sci USA*. 2007;104:11418–11423. doi: 10.1073/pnas.0610467104
- Paulin R, Michelakis ED. The metabolic theory of pulmonary arterial hypertension. *Circ Res*. 2014;115:148–164. doi: 10.1161/CIRCRESAHA.115.301130
- Okada-Iwabu M, Yamauchi T, Iwabu M, et al. A small-molecule AdipoR agonist for type 2 diabetes and short life in obesity. *Nature*. 2013;503:493–499. doi: 10.1038/nature12656
- Kikuchi H, Sekiya M, Katou Y, Ueda K, Kabeya T, Kurata S, Oshima Y. Revised structure and synthesis of celastramycin a, a potent innate immune suppressor. *Org Lett*. 2009;11:1693–1695. doi: 10.1021/ol9002306
- Yajima M, Takada M, Takahashi N, Kikuchi H, Natori S, Oshima Y, Kurata S. A newly established in vitro culture using transgenic *Drosophila* reveals functional coupling between the phospholipase A2-generated fatty acid cascade and lipopolysaccharide-dependent activation of the immune deficiency (*imd*) pathway in insect immunity. *Biochem J*. 2003;371:205–210. doi: 10.1042/BJ20021603

13. Tomita T, Ieguchi K, Coin F, Kato Y, Kikuchi H, Oshima Y, Kurata S, Maru Y. ZFC3H1, a zinc finger protein, modulates IL-8 transcription by binding with celsastramycin A, a potential immune suppressor. *PLoS One*. 2014;9:e108957. doi: 10.1371/journal.pone.0108957
14. Vergadi E, Chang MS, Lee C, Liang OD, Liu X, Fernandez-Gonzalez A, Mitsialis SA, Kourembanas S. Early macrophage recruitment and alternative activation are critical for the later development of hypoxia-induced pulmonary hypertension. *Circulation*. 2011;123:1986–1995. doi: 10.1161/CIRCULATIONAHA.110.978627
15. Fessel JP, West JD. Redox biology in pulmonary arterial hypertension (2013 Grover Conference Series). *Pulm Circ*. 2015;5:599–609. doi: 10.1086/683814
16. Sutendra G, Dromparis P, Bonnet S, Haromy A, McMurtry MS, Bleackley RC, Michelakis ED. Pyruvate dehydrogenase inhibition by the inflammatory cytokine TNF α contributes to the pathogenesis of pulmonary arterial hypertension. *J Mol Med*. 2011;89:771–783. doi: 10.1007/s00109-011-0762-2
17. Satoh K, Satoh T, Kikuchi N, et al. Basigin mediates pulmonary hypertension by promoting inflammation and vascular smooth muscle cell proliferation. *Circ Res*. 2014;115:738–750. doi: 10.1161/CIRCRESAHA.115.304563
18. Omura J, Satoh K, Kikuchi N, et al. Protective roles of endothelial AMP-activated protein kinase against hypoxia-induced pulmonary hypertension in mice. *Circ Res*. 2016;119:197–209. doi: 10.1161/CIRCRESAHA.115.308178
19. Kikuchi N, Satoh K, Kurosawa R, Yaoita N, Elias-Al-Mamun M, Siddique MAH, Omura J, Satoh T, Nogi M, Sunamura S, Miyata S, Saito Y, Hoshikawa Y, Okada Y, Shimokawa H. Selenoprotein P promotes the development of pulmonary arterial hypertension. *Circulation*. 2018;138:600–623. doi: 10.1161/CIRCULATIONAHA.117.033113
20. Bonnet S, Provencher S, Guignabert C, Perros F, Boucherat O, Schermuly RT, Hassoun PM, Rabinovitch M, Nicolls MR, Humbert M. Translating research into improved patient care in pulmonary arterial hypertension. *Am J Respir Crit Care Med*. 2017;195:583–595. doi: 10.1164/rccm.201607-1515PP
21. Provencher S, Archer SL, Ramirez FD, Hibbert B, Paulin R, Boucherat O, Lacasse Y, Bonnet S. Standards and methodological rigor in pulmonary arterial hypertension preclinical and translational research. *Circ Res*. 2018;122:1021–1032. doi: 10.1161/CIRCRESAHA.117.312579
22. Meloche J, Pflieger A, Vaillancourt M, Paulin R, Potus F, Zervopoulos S, Graydon C, Courboulain A, Breuils-Bonnet S, Tremblay E, Couture C, Michelakis ED, Provencher S, Bonnet S. Role for DNA damage signaling in pulmonary arterial hypertension. *Circulation*. 2014;129:786–797. doi: 10.1161/CIRCULATIONAHA.113.006167
23. Efron B, Tibshirani RJ. *An Introduction to the Bootstrap*. London, NY: Chapman and Hall Ltd; 1993.
24. Bretz F, Hothorn T, Westfall P. *Multiple Comparisons Using R*. London, UK: Chapman and Hall/CRC. 2010.
25. Shimizu T, Fukumoto Y, Tanaka S, Satoh K, Ikeda S, Shimokawa H. Crucial role of ROCK2 in vascular smooth muscle cells for hypoxia-induced pulmonary hypertension in mice. *Arterioscler Thromb Vasc Biol*. 2013;33:2780–2791. doi: 10.1161/ATVBAHA.113.301357
26. Dabral S, Tian X, Kojonazarov B, Savai R, Ghofrani HA, Weissmann N, Florio M, Sun J, Jonigk D, Maegel L, Grimminger F, Seeger W, Savai Pullamsetti S, Schermuly RT. Notch1 signalling regulates endothelial proliferation and apoptosis in pulmonary arterial hypertension. *Eur Respir J*. 2016;48:1137–1149. doi: 10.1183/13993003.00773-2015
27. Sunamura S, Satoh K, Kurosawa R, et al. Different roles of myocardial ROCK1 and ROCK2 in cardiac dysfunction and postcapillary pulmonary hypertension in mice. *Proc Natl Acad Sci USA*. 2018;115:E7129–E7138. doi: 10.1073/pnas.1721298115
28. Nogi M, Satoh K, Sunamura S, et al. SmgGDS prevents thoracic aortic aneurysm formation and rupture by phenotypic preservation of aortic smooth muscle cells. *Circulation*. 2018;138:2413–2433. doi: 10.1161/CIRCULATIONAHA.118.035648
29. Bonnet S, Michelakis ED, Porter CJ, Andrade-Navarro MA, Thebaud B, Bonnet S, Haromy A, Harry G, Moudgil R, McMurtry MS, Weir EK, Archer SL. An abnormal mitochondrial-hypoxia inducible factor-1 α -Kv channel pathway disrupts oxygen sensing and triggers pulmonary arterial hypertension in fawn hooded rats: similarities to human pulmonary arterial hypertension. *Circulation*. 2006;113:2630–2641. doi: 10.1161/CIRCULATIONAHA.105.609008
30. Papaiahgari S, Kleeberger SR, Cho HY, Kalvakolanu DV, Reddy SP. NADPH oxidase and ERK signaling regulates hyperoxia-induced Nrf2-ARE transcriptional response in pulmonary epithelial cells. *J Biol Chem*. 2004;279:42302–42312. doi: 10.1074/jbc.M408275200
31. Brewer AC, Murray TV, Arno M, Zhang M, Anilkumar NP, Mann GE, Shah AM. Nox4 regulates Nrf2 and glutathione redox in cardiomyocytes in vivo. *Free Radic Biol Med*. 2011;51:205–215. doi: 10.1016/j.freeradbiomed.2011.04.022
32. Kovac S, Angelova PR, Holmström KM, Zhang Y, Dinkova-Kostova AT, Abramov AY. Nrf2 regulates ROS production by mitochondria and NADPH oxidase. *Biochim Biophys Acta*. 2015;1850:794–801. doi: 10.1016/j.bbagen.2014.11.021
33. Sutendra G, Michelakis ED. The metabolic basis of pulmonary arterial hypertension. *Cell Metab*. 2014;19:558–573. doi: 10.1016/j.cmet.2014.01.004
34. Rhodes CJ, Ghataorhe P, Wharton J, et al. Plasma metabolomics implicates modified transfer RNAs and altered bioenergetics in the outcomes of pulmonary arterial hypertension. *Circulation*. 2017;135:460–475. doi: 10.1161/CIRCULATIONAHA.116.024602
35. Ogawa A, Firth AL, Yao W, Rubin LJ, Yuan JX. Prednisolone inhibits PDGF-induced nuclear translocation of NF- κ B in human pulmonary artery smooth muscle cells. *Am J Physiol Lung Cell Mol Physiol*. 2008;295:L648–L657. doi: 10.1152/ajplung.90245.2008
36. Meloche J, Potus F, Vaillancourt M, et al. Bromodomain-containing protein 4: the epigenetic origin of pulmonary arterial hypertension. *Circ Res*. 2015;117:525–535. doi: 10.1161/CIRCRESAHA.115.307004
37. Hussong M, Börno ST, Kerick M, Wunderlich A, Franz A, Sülthmann H, Timmermann B, Lehrach H, Hirsch-Kauffmann M, Schweiger MR. The bromodomain protein BRD4 regulates the KEAP1/NRF2-dependent oxidative stress response. *Cell Death Dis*. 2014;5:e1195. doi: 10.1038/cddis.2014.157
38. Michaeloudes C, Mercado N, Clarke C, Bhavsar PK, Adcock IM, Barnes PJ, Chung KF. Bromodomain and extraterminal proteins suppress NF-E2-related factor 2-mediated antioxidant gene expression. *J Immunol*. 2014;192:4913–4920. doi: 10.4049/jimmunol.1301984
39. Ranchoux B, Meloche J, Paulin R, Boucherat O, Provencher S, Bonnet S. DNA damage and pulmonary hypertension. *Int J Mol Sci*. 2016;17:E990. doi: 10.3390/ijms17060990
40. Meola N, Domanski M, Karadoulama E, Chen Y, Gentil C, Pultz D, Vitting-Seerup K, Lykke-Andersen S, Andersen JS, Sandelin A, Jensen TH. Identification of a nuclear exosome decay pathway for processed transcripts. *Mol Cell*. 2016;64:520–533. doi: 10.1016/j.molcel.2016.09.025
41. Lee NN, Chalamcharla VR, Reyes-Turcu F, Mehta S, Zofall M, Balachandran V, Dhakshnamoorthy J, Taneja N, Yamanaka S, Zhou M, Grewal SL. Mtr4-like protein coordinates nuclear RNA processing for heterochromatin assembly and for telomere maintenance. *Cell*. 2013;155:1061–1074. doi: 10.1016/j.cell.2013.10.027
42. Chlebowski A, Lubas M, Jensen TH, Dziembowski A. RNA decay machines: the exosome. *Biochim Biophys Acta*. 2013;1829:552–560. doi: 10.1016/j.bbagr.2013.01.006
43. Ryan JJ, Marsboom G, Fang YH, Toth PT, Morrow E, Luo N, Piao L, Hong Z, Ericson K, Zhang HJ, Han M, Hancy CR, Chen CT, Sharp WW, Archer SL. PGC1 α -mediated mitofusin-2 deficiency in female rats and humans with pulmonary arterial hypertension. *Am J Respir Crit Care Med*. 2013;187:865–878. doi: 10.1164/rccm.201209-1687OC
44. Fernandez-Marcos PJ, Auwerx J. Regulation of PGC-1 α , a nodal regulator of mitochondrial biogenesis. *Am J Clin Nutr*. 2011;93:884S–889S. doi: 10.3945/ajcn.110.001917
45. Wan Z, Root-McCaig J, Castellani L, Kemp BE, Steinberg GR, Wright DC. Evidence for the role of AMPK in regulating PGC-1 α expression and mitochondrial proteins in mouse epididymal adipose tissue. *Obesity (Silver Spring)*. 2014;22:730–738. doi: 10.1002/oby.20605
46. Rabinovitch RC, Samborska B, Faubert B, Ma EH, Gravel SP, Andrzejewski S, Raissi TC, Pause A, St-Pierre J, Jones RG. AMPK maintains cellular metabolic homeostasis through regulation of mitochondrial reactive oxygen species. *Cell Rep*. 2017;21:1–9. doi: 10.1016/j.celrep.2017.09.026
47. Bonnet S, Paulin R, Boucherat O. Small SeP or giant leap for pulmonary hypertension research? *Circulation*. 2018;138:624–626. doi: 10.1161/CIRCULATIONAHA.118.035427
48. Kikuchi N, Satoh K, Saito Y, Shimokawa H. Response by kikuchi et al regarding article, “selenoprotein P promotes the development of pulmonary arterial hypertension: a possible novel therapeutic target”. *Circulation*. 2018;139:724–725. doi: 10.1161/CIRCULATIONAHA.117.033113
49. Pullen C, Schmitz P, Meurer K, Bamberg DD, Lohmann S, De Castro França S, Groth I, Schlegel B, Möllmann U, Gollmick F, Gräfe U, Leistner E. New and bioactive compounds from *Streptomyces* strains residing in the wood of Celastraceae. *Planta*. 2002;216:162–167. doi: 10.1007/s00425-002-0874-6

50. Voelkel NF, Tuder RM, Bridges J, Arend WP. Interleukin-1 receptor antagonist treatment reduces pulmonary hypertension generated in rats by monocrotaline. *Am J Respir Cell Mol Biol*. 1994;11:664–675. doi: 10.1165/ajrcmb.11.6.7946395
51. Hashimoto-Kataoka T, Hosen N, Sonobe T, et al. Interleukin-6/interleukin-21 signaling axis is critical in the pathogenesis of pulmonary arterial hypertension. *Proc Natl Acad Sci USA*. 2015;112:E2677–E2686. doi: 10.1073/pnas.1424774112
52. Bauer EM, Chanthaphavong RS, Sodhi CP, Hackam DJ, Billiar TR, Bauer PM. Genetic deletion of toll-like receptor 4 on platelets attenuates experimental pulmonary hypertension. *Circ Res*. 2014;114:1596–1600. doi: 10.1161/CIRCRESAHA.114.303662
53. Chen CY, Gherzi R, Ong SE, Chan EL, Raijmakers R, Puijn GJ, Stoecklin G, Moroni C, Mann M, Karin M. AU binding proteins recruit the exosome to degrade ARE-containing mRNAs. *Cell*. 2001;107:451–464.
54. Suzuki T, Shibata T, Takaya K, Shiraishi K, Kohno T, Kunitoh H, Tsuta K, Furuta K, Goto K, Hosoda F, Sakamoto H, Motohashi H, Yamamoto M. Regulatory nexus of synthesis and degradation deciphers cellular Nrf2 expression levels. *Mol Cell Biol*. 2013;33:2402–2412. doi: 10.1128/MCB.00065-13
55. Eba S, Hoshikawa Y, Moriguchi T, Mitsuishi Y, Satoh H, Ishida K, Watanabe T, Shimizu T, Shimokawa H, Okada Y, Yamamoto M, Kondo T. The nuclear factor erythroid 2-related factor 2 activator oltipraz attenuates chronic hypoxia-induced cardiopulmonary alterations in mice. *Am J Respir Cell Mol Biol*. 2013;49:324–333. doi: 10.1165/rcmb.2011-0396OC
56. Sutendra G, Michelakis ED. Pulmonary arterial hypertension: challenges in translational research and a vision for change. *Sci Transl Med*. 2013;5:208sr5
57. Paulin R, Dromparis P, Sutendra G, Gurtu V, Zervopoulos S, Bowers L, Haromy A, Webster L, Provencher S, Bonnet S, Michelakis ED. Sirtuin 3 deficiency is associated with inhibited mitochondrial function and pulmonary arterial hypertension in rodents and humans. *Cell Metab*. 2014;20:827–839. doi: 10.1016/j.cmet.2014.08.011
58. Bonnet S, Archer SL, Allalunis-Turner J, et al. A mitochondria-K⁺ channel axis is suppressed in cancer and its normalization promotes apoptosis and inhibits cancer growth. *Cancer Cell*. 2007;11:37–51. doi: 10.1016/j.ccr.2006.10.020
59. Archer SL. Mitochondrial dynamics—mitochondrial fission and fusion in human diseases. *N Engl J Med*. 2013;369:2236–2251. doi: 10.1056/NEJMr1215233
60. Hu J, Xu Q, McTiernan C, Lai YC, Osei-Hwedieh D, Gladwin M. Novel targets of drug treatment for pulmonary hypertension. *Am J Cardiovasc Drugs*. 2015;15:225–234. doi: 10.1007/s40256-015-0125-4